JOURNAL OF VIROLOGY, Dec. 2003, p. 12507–12522 Vol. 77, No. 23
0022-538X/03/$08.00+0 DOI: 10.1128/JVI.77.23.12507–12522.2003

The Human *Polycomb* Group EED Protein Interacts with the Integrase of Human Immunodeficiency Virus Type 1

Sébastien Violot,[1] Saw See Hong,[1] Dina Rakotobe,[1] Caroline Petit,[2]† Bernard Gay,[1]‡ Karen Moreau,[1]§ Geneviève Billaud,[1] Stéphane Priet,[3] Joséphine Sire,[3] Olivier Schwartz,[2] Jean-François Mouscadet,[4] and Pierre Boulanger[1]*

Laboratoire de Virologie and Pathogénèse Virale, Faculté de Médecine RTH Laennec, CNRS UMR-5537 and Université Claude Bernard Lyon 1, 69372 Lyon Cedex 08,[1] Laboratoire Rétrovirus et Transfert Génétique, Institut Pasteur, 75724 Paris Cedex 15,[2] Unité de Pathogénie des Infections à Lentivirus, INSERM U-372, 13276 Marseille Cedex 09,[3] and CNRS UMR-8532, Ecole Normale Supérieure, 94235 Cachan Cedex,[4] France

Received 21 April 2003/Accepted 23 August 2003

Human EED, a member of the superfamily of WD-40 repeat proteins and of the *Polycomb* group proteins, has been identified as a cellular partner of the human immunodeficiency virus type 1 (HIV-1) matrix (MA) protein (R. Peytavi et al., J. Biol. Chem. 274:1635-1645, 1999). In the present study, EED was found to interact with HIV-1 integrase (IN) both in vitro and in vivo in yeast. In vitro, data from mutagenesis studies, pull-down assays, and phage biopanning suggested that EED-binding site(s) are located in the C-terminal domain of IN, between residues 212 and 264. In EED, two putative discrete IN-binding sites were mapped to its N-terminal moiety, at a distance from the MA-binding site, but EED-IN interaction also required the integrity of the EED last two WD repeats. EED showed an apparent positive effect on IN-mediated DNA integration reaction in vitro, in a dose-dependent manner. In situ analysis by immunoelectron microscopy (IEM) of cellular distribution of IN and EED in HIV-1-infected cells (HeLa CD4$^+$ cells or MT4 lymphoid cells) showed that IN and EED colocalized in the nucleus and near nuclear pores, with maximum colocalization events occurring at 6 h postinfection (p.i.). Triple colocalizations of IN, EED, and MA were also observed in the nucleoplasm of infected cells at 6 h p.i., suggesting the ocurrence of multiprotein complexes involving these three proteins at early steps of the HIV-1 virus life cycle. Such IEM patterns were not observed with a noninfectious, envelope deletion mutant of HIV-1.

Integration of the proviral DNA into the host cell genome has been considered an obligatory step of the human immunodeficiency virus type 1 (HIV-1) life cycle, as for all known retroviruses (20, 35). The host DNA sites for retroviral integration have been long debated. Although it has been reported that integration events are statistically more frequent in inactive than active chromatin (11, 81, 82), other data suggest that retrovirus integration preferentially occurs in transcriptionally active chromatin (65) and in regions of DNA distortion (57–59). Recent studies have confirmed that transcriptional units are preferred targets for both murine leukemia virus (MLV) and HIV-1 (66, 83), but refined mapping of integration sites has revealed significant differences between HIV-1 and MLV, the latter preferentially integrating near the start of transcription (83). Whatever the scenario followed by the different types of retroviruses in their host cells, it is reasonable to assume that proteins which control the state of cellular chromatin would play a key role in the integration of HIV proviral DNA and, possibly, in further steps of the virus life cycle. The viral RNA genome is retrotranscribed by the reverse transcriptase (RT) into a double-stranded DNA molecule, which is the substrate for the viral integrase (IN) in the integration reaction. The RT reaction starts within the central core of extracellular virions, before they bind to the surface of the host cell, and is completed after the virus enters the cell (reviewed in references 5, 30, and 35). The final reaction takes place after partial uncoating of the HIV-1 particle, within a protein-nucleic acid complex termed preintegration complex (PIC). PIC competent for integration reaction in vitro has been isolated from HIV-1-infected cells (20, 43, 48, 49).

It is generally recognized that PIC is composed of linear double-stranded DNA, RT, IN, matrix protein (MA), nucleocapsid protein (NC), and auxiliary protein Vpr (reviewed in references 13, 16, 30, and 71). One of these components, the MA protein, has been identified as an effector of various biological functions in the virus life cycle (reviewed in reference 23). Since the MA carries a potential nuclear localization signal, it has been hypothesized to mediate the transport of PIC to the cell nucleus and its traverse of the nuclear pore complex (6, 7, 26, 27). However, the observation that a mutant HIV-1 virus with most of the MA domain deleted was still capable of infecting nondividing cells (60) argued against a major role of the basic MA sequences in the nuclear import of the PIC, and other data seem to assign this function to the Vpr protein (13,

* Corresponding author. Mailing address: Laboratoire de Virologie and Pathogénèse Virale, Faculté de Médecine RTH Laennec de Lyon, 7, Rue Guillaume Paradin, 69372 Lyon Cedex 08, France. Phone: 33-4-7877-8621. Fax: 33-4-7877-8751. E-mail: Pierre.Boulanger@laennec.univ-lyon1.fr.

† Present address: Institut Cochin de Génétique Moléculaire, 75014 Paris, France.

‡ Present address: Laboratoire Infections Rétrovirales et Signalisation Cellulaire, CNRS UMR 5121, Institut de Biologie, 34060 Montpellier, France.

§ Present address: Laboratoire Génétique et Cancer, CNRS UMR 5641 and Université Claude Bernard Lyon 1, 69373 Lyon Cedex 08, France.

16, 22, 71), IN (2, 52), and the central DNA flap (18, 85). Several cellular proteins such as high-mobility-group proteins (19, 28), the barrier-to-autointegration factor (41), IN interactor 1 (Ini1) (40, 48, 84), and human lens epithelium-derived growth factor (LEDGF/p75) (45), have been identified as partners of IN and/or cofactors of integration reaction, and at least one of them, the barrier-to-autointegration factor, has been found to be associated with PIC of MLV and HIV-1 (43, 77). These proteins could participate, directly or indirectly, in the cellular trafficking of PIC and/or in provirus integration.

One of the cellular partners of the HIV-1 MA protein has been identified as EED (54), the human homolog of the mouse embryonic ectoderm development (*eed*) gene product (51, 67, 68, 74), and a member of the WD-40 repeat superfamily of proteins (50). The *eed* gene is highly conserved in humans and mice and is also homologous to the *Drosophila esc* gene. Both *eed* and *esc* belong to the family of widely conserved *Polycomb* group (*Pc*-G) of genes (17, 51). EED and many other proteins of the *Pc*-G family act as transcriptional repressors and gene silencers (1, 3, 17, 64, 67, 68, 74). The product of the *Pc*-G genes in eukaryotes are involved in chromatin remodeling and, in particular, in the maintenance of the silent state of chromatin (reviewed in reference 55) and the reduction of DNA accessibility (21). EED has also been found to colocalize with histone H1 in heterochromatin subdomains of neuronal cell nuclei containing inactive DNA (1).

Previous studies have indicated that MA, RT, and IN proteins are each a component of HIV-1 PIC (26, 27, 49). Since MA has been found to bind to cellular EED (54), we explored the possibility of a protein-protein interaction between EED and IN and of the occurrence of a ternary complex of EED, MA, and IN. We found that IN and EED proteins were indeed able to interact in vitro, as well as in vivo, in yeast. In human cells infected with HIV-1 (HeLa $CD4^+$ cells or MT4 lymphoid cells), in situ analysis by immunoelectron microscopy (IEM) showed that EED, IN, and MA proteins colocalized within the nucleus, with a maximum number of colocalization events occurring at 6 h after infection. Such patterns of nuclear colocalization were not observed in cells incubated with a noninfectious, envelope deletion mutant of HIV-1. Our data suggest that EED, a cellular partner of both MA and IN, would play a functional role in the HIV-1 life cycle, acting at early steps of virus infection.

MATERIALS AND METHODS

Cells, HIV-1 viruses and virus infection. Human embryonic kidney cells (HEK-293) and epithelial cells (P4P56) (HeLa $CD4^+$, *lck*+, LTR-*LacZ*) (52) were grown in Dulbecco modified Eagle medium (Gibco), supplemented with glutamine, antibiotics, and 10% fetal calf serum. MT4 lymphoid cells were grown in RPMI medium with the same supplements. The construction of HIV-1 BRU infectious molecular clone expressing the viral IN fused to the Flag epitope has been described in a previous study (53). It is abbreviated as BRU-FlagWT in the present study. BRU-FlagΔEnv mutant was derived from the BRU-Flag virus, by a deletion in the *env* gene (*Kpn*I-*Bgl*II, nucleotides 6343 to 7600 of the sequence of the NL43/2 clone). Viruses were produced by transfection of the corresponding plasmids as previously described (69). Supernatants were analyzed for HIV-1 p24 antigen content, and infectivity titers are expressed here in nanograms of p24 per milliliter (53). Aliquots of MT4 and P4P56 cell samples (4×10^6 cells) were infected at a multiplicity of infection of 150 ng of p24 antigen per 10^6 cells, i.e., ca. 1,000 virus particles per cell, considering the latest estimate of 4,000 to 5,000 copies of CA per HIV-1 virion. In negative control experiments, cells were treated with 15 μM zidovudine (AZT), which was added 3 h before infection and maintained throughout the infection period. Cells were harvested at 0 (mock-infected cells), 1.5, 6, and 24 h postinfection (p.i.); fixed in 0.5% glutaraldehyde–4% paraformaldehyde; and processed for IEM.

Yeast two-hybrid assays. (i) Generation of the DNA-binding LexA-IN hybrid (Fig. 1A). The portion of the HIV-1_{BRU} *pol* gene segment coding for the IN was cloned in frame with the DNA-binding *LexA* gene into the pBTM116 vector (47). The sequence of the construct was verified by DNA sequencing, and the expression of recombinant fusion protein in yeast was confirmed by gel electrophoresis and immunoblot analysis with anti-IN polyclonal antibody as described below. (ii) Generation of the pGAD-EED (Fig. 1A). The cDNA of wild-type (WT) EED (54) was inserted into the *Eco*RI and *Not*I sites of the Gal4 transcription activation domain vector pGAD3S2X, a modified version of the pGAD GH (Clontech) containing a *Not*I site in its polylinker. This resulted in a Gal4 activation domain AD-EED hybrid. In the hybrid mutant AD-EED-305A4 the tetrapeptide motif HNRY from positions 305 to 308 was replaced by the tetrapeptide AAAA, and in AD-EED-300AI the dipeptide motif ST at positions 300 and 301 was replaced by AI. (iii) The two-hybrid assays were performed as described in a previous study (54).

Bacterially expressed IN and EED recombinant proteins. The full-length, WT HIV-1 BRU IN, and various deletion mutants of IN were expressed in bacteria as glutathione *S*-transferase (GST) fusion proteins (GST-IN) (56). Their schematic structure and domains are presented in Fig. 1B, along with their acronyms. Likewise, full-length WT human EED was expressed as a GST fusion protein (GST-EED-441) by using the pGEX-KG plasmid (32). EED C-terminal deletion mutant was generated by insertion of a TGA stop codon at position 349 of GST-EED-441, yielding mutant protein GST-EED-C348. In the substitution mutant GST-EED-103A3, the tripeptide motif WHS from positions 103 to 105 was replaced by the tripeptide AAA. Various forms of EED and IN were also also expressed as His_6-tagged proteins (Fig. 1B) by using the pT7-7 IPTG-inducible promoter (14). This was the case for the full-length versions of EED (tagged at its C terminus and abbreviated EED-441-H6) and of IN (tagged at its N terminus and abbreviated H6-IN-WT) and for the N and C terminally deleted versions of IN (abbreviated H6-IN-ΔN and H6-IN-ΔC, respectively). Mutagenesis was performed by using PCR and splicing by overlap extension (34, 38). Mutant sequences were verified by DNA sequencing.

Purification of recombinant tagged proteins and affinity pull-down assays. Bacterial cells expressing the desired protein were centrifuged and resuspended at 1 to 2 g (wet weight) per 2 to 5 ml of lysis buffer (10 mM Tris-HCl [pH 8.0], 5 mM $MgCl_2$, 1 mM EDTA, 1% Triton X-100, 1 mM phenylmethylsulfonyl fluoride) and then disrupted by sonication. After incubation for 30 min in the presence of a broad-spectrum endonuclease (*Serratia marcescens* Benzonase; Sigma) at 100 U/ml of sample, the lysates were clarified by centrifugation at $100{,}000 \times g$ for 45 min. GST fusion proteins were purified by adsorption on a glutathione-Sepharose gel and recovered by elution with a glutathione-containing buffer or by thrombin cleavage of the GST linker by using a commercial kit (Bulk GST Purification Module; Pharmacia Biotech). For purification of His-tagged proteins, the bacterial cell lysate supernatant was applied to a Ni^{2+}-nitrilotriacetic acid (NTA)-agarose column (Qiagen, Inc.) equilibrated in sodium phosphate buffer (SPB; 16 mM Na_2HPO_4, 4 mM NaH_2PO_4 [pH 6.8]) containing 0.5 M NaCl (SPB-500) and 1% Triton X-100. Unbound and weakly adsorbed proteins were washed from the affinity gel with 10 column volumes of SPB-500 containing 5 and 30 mM imidazole, successively, and then His-tagged proteins were eluted at 250 mM imidazole in SPB-500. For in vitro binding reactions, 100-ml cultures of *Escherichia coli* expressing GST fusion protein were centrifuged, resuspended in 400-μl aliquots of binding buffer (BB; phosphate-buffered saline containing 0.2% Nonidet P-40 and a cocktail of protease inhibitors [Boehringer Mannheim]), sonicated, and clarified by centrifugation. Aliquots (20 μl) of a glutathione-Sepharose bead suspension were added to the bacterial cell lysates, followed by incubation for 30 min at 4°C. After an extensive rinsing in BB, the affinity beads were mixed with 100 to 200 μl (100 μg of total protein) of cell lysates (from bacteria or insect cells) containing nontagged or differentially tagged partner protein and 900 μl of BB, followed by incubation for 2 h at room temperature. The beads were then washed three times with 500 μl of BB, resuspended, and boiled in 50 μl of sodium dodecyl sulfate (SDS) sample buffer. Alternatively, His-tagged proteins were retained on Ni^{2+}-NTA-agarose beads, and affinity beads were processed as described above by using a magnetic pull-down device (Qiagen). Protein pull-down experiments were also performed with affinity-purified proteins, e.g., GST-IN plus EED-441-H6 or H6-IN-WT plus GST-EED. Pull-down proteins were analyzed by SDS-polyacrylamide gel electrophoresis (PAGE) and immunoblotting.

Gel electrophoresis and immunoblotting analysis. PAGE of SDS-denatured protein samples and immunoblotting analysis have been described in detail in previous studies (8, 12, 54). Briefly, proteins were electrophoresed in SDS–

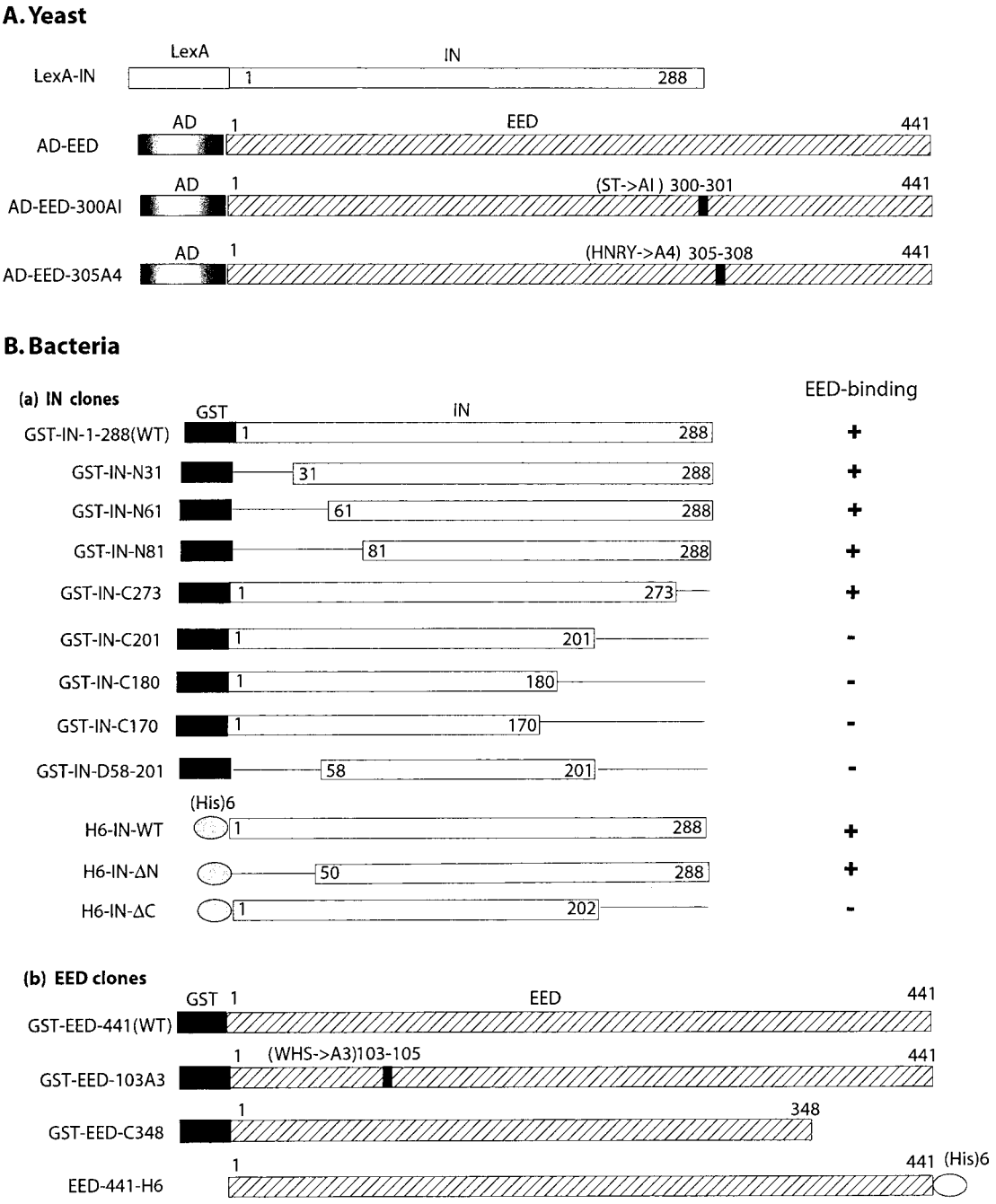

FIG. 1. Schematic representation of genetic constructs of HIV-1 IN and EED, expressed in yeast (A) or in bacteria (B). The LexA (DNA-binding) domain and the Gal4 activating domain (AD) are shown by gray boxes, the GST domain by a black box, the His_6 tag by a gray ellipse, the IN sequence by an open box, and EED by a hatched box. In panel Ba, deletions in the IN sequence are represented by a solid line. In panels A and Bb, the point mutations in the EED protein are shown as black bars, with the mutated amino acids indicated above. On the right of panel Ba, the binding of EED to IN protein (WT or deletants) is indicated by "+" or a "−."

denaturing, 10% polyacrylamide gel and electrically transferred to nitrocellulose membrane. Blots were blocked in 5% skimmed milk in Tris-buffered saline (TBS) containing 0.05% Tween 20 (TBS-T), rinsed in TBS-T, and then successively incubated with primary rabbit or mouse antibody (working dilutions of 1:1,000 to 1:2,000) and the complementary peroxidase- or phosphatase-labeled anti-immunoglobulin G (IgG) conjugate (1:1,000).

Antibodies. For detection of EED, IN, and MA proteins by blotting, immunofluorescence, or IEM, the following antibodies were used. Antiserum against EED was prepared in rabbits by injection of affinity-purified EED protein (54). Anti-IN rabbit polyclonal antibody was also laboratory-made (42), as well as our anti-GST rabbit antiserum. For Flag-tagged IN (53), mouse monoclonal antibody (MAb) anti-Flag M2 (Kodak) or rabbit polyclonal anti-Flag (Zymed Laboratories, South San Francisco, Calif.) were used. MA protein was detected with MAb anti-MAp17 (Epiclone 5003 [Cylex, Inc., Columbia, Md.] mapped to epitope 121-DTGHSSQVSQNY-132) (12) or rabbit polyclonal anti-MA antibody (laboratory-made) (39). His-tagged proteins were detected by using monoclonal anti-His.Tag antibody (Novagen) specific for N-terminal, C-terminal, and internal histidine clusters.

Phage-displayed peptide libraries and biopanning. Two filamentous phage-displayed peptide libraries were used, one consisting of random hexapeptides

(kindly provided by G. Smith [75]), the other of dodecapeptides (BioLabs). Biopanning of immobilized protein ligate and specific ligand elution of phages have been described in previous studies (36, 37, 39). Purified protein (e.g., IN) was immobilized on enzyme-linked immunosorbent assay plates used as the solid support. Elution of phages was carried out by using the purified partner protein as a soluble competing ligand (in this case, EED). In the reverse biopanning experiment, purified EED was coated onto the plate, and IN was used as the soluble competing ligand. The hexapeptide or dodecapeptide phagotopes were identified by manual DNA sequencing of the recombinant fUSE5 pIII protein (36, 37) by using the dideoxynucleotide chain termination method, the required oligonucleotide primers, and the Sequenase kit version 2.0 (Amersham Biosciences).

In vitro HIV-1 IN assays. Recombinant, bacterially expressed, N-terminally His-tagged HIV-1 IN protein was purified by affinity chromatography (44). IN-mediated strand transfer was assayed in vitro by using a restriction fragment from a modified version of plasmid pU3U5 ((9) as the IN substrate (donor DNA) and plasmid pBSK-*zeo* (a 3-kbp pBSK-derived construct in which the *amp* gene has been replaced by the *zeocine-resistance* gene) as target DNA. The donor DNA (300-bp fragment) contained the 20 terminal base pairs of the HIV-1 5′ and 3′ long terminal repeat (LTR) at each ends, with two-base 5′ overhangs generated by *Nde*I cleavage. Integration reactions (20 μl, final volume) were performed by using 10 ng of ^{32}P-labeled donor DNA, 100 ng of target DNA, and 2 to 5 pmol of IN (200 to 500 nM, final concentration) in 20 mM HEPES (pH 7.5) buffer containing 50 mM NaCl, 30 mM $MgCl_2$, 1 mM dithiothreitol, 15% dimethyl sulfoxide, and 8% PEG-8000. EED and IN proteins (diluted in reaction buffer) were mixed and preincubated at 0°C for 30 min in molar ratios varying from 1:0.5 to 1:16 in terms of IN:EED stoichiometry. Control reactions were performed with mock samples consisting of the same chromatographic fraction as the one containing IN but from bacterial lysates harboring a void plasmid. Donor and target DNAs were incubated with protein mix for an additional 30 min at 0°C. Reaction buffer was then added to the mixture to a final volume of 20 μl, and the reaction was allowed to proceed for 90 min at 37°C. Reaction products were phenol extracted, ethanol precipitated, and electrophoresed in 1.2% agarose gels. Agarose gels were dried, autoradiographed, and quantitatively analyzed by using a PhosphorImager SI-475 (Molecular Dynamics).

EM and IEM. Cell specimens were included in metacrylate resin, sectioned and processed for conventional electron microscopy (EM) or IEM according to previously described methods (8, 29, 54). Cellular localization and possible co-localization of EED, IN, and MA proteins were analyzed in HIV-infected cells at different times p.i. by using single, double, or triple labeling with the relevant primary antibody, followed by the corresponding (anti-mouse or anti-rabbit IgG) colloidal gold-conjugated complementary antibodies. For IEM, rabbit IgG from laboratory-made antisera was purified by affinity chromatography by using a protein A-Sepharose column. MA protein was detected by using mouse monoclonal or rabbit polyclonal anti-MA antibodies, EED with rabbit antibody, and IN with anti-Flag MAb or rabbit anti-IN. In double-labeling experiments, when a 5-nm-gold-conjugated anti-mouse IgG antibody was used, a 10-, a 15-, or a 20-nm-gold-conjugated anti-rabbit IgG antibody was simultaneously used on the same cell section. In the triple-labeling experiments, since two primary antibodies belonged to the same species (e.g., the two rabbit anti-MA and anti-EED antibodies), both sides of the specimens on the grids were successively reacted. One side was simultaneously incubated with anti-MA rabbit antibody and anti-Flag(IN) MAb, followed by 10-nm-gold-conjugated anti-rabbit IgG antibody and 5-nm-gold-conjugated anti-mouse IgG antibody. The other side was then incubated with anti-EED rabbit antibody, followed by 20-nm-gold-conjugated anti-rabbit IgG antibody. To verify that there was no undesired cross-reaction of the 20-nm-gold-conjugated anti-rabbit IgG antibody with primary rabbit IgG bound to antigens on the first side of the section, stereoscopic views were taken upon tilting of the microscope goniometer. The 20-nm-gold grains could be seen, by using stereoscopic glasses, in a plane different from that of 5- and 10-nm gold grains (as exemplified in Fig. 9). Specimens were examined under a Hitachi HU7001 or a JEOL 1200-EX electron microscope, the latter equipped with a MegaView II High-Resolution TEM camera and a Soft Imaging System of analysis (Eloïse, Roissy, France).

RESULTS

The larger isoform of human EED protein is now considered to be comprised of 441 residues. An ortholog of human and murine EED has been identified in *Xenopus* and is called Xeed (73). As in human EED, the initiator methionine in Xeed corresponds to the Met95 codon in the murine ortholog (mEED) sequence and terminates at residue Arg441, corresponding to Arg535 in mEED (17, 54). From sequence analogy with insect ESC proteins and mammalian Gβ protein (51), the full-length sequence of EED larger isoform contains seven potential WD repeats (54). Compared to WT EED, mutant EED-Ct348 had lost its last two WD repeats. (see Fig. 1 and the legend to Table 2).

Interaction of human EED protein with HIV-1 IN in yeast two-hybrid assays. The HIV-1_{BRU} IN, fused to the DNA-binding LexA protein (BD hybrid), was used in yeast two-hybrid assays to test the possible interaction with EED protein, coexpressed as the Gal4 transcription activation domain-fusion protein AD-EED. WT EED and IN proteins interacted in yeast with a significant affinity (Fig. 2A), which was ~2-fold lower than that shown by the strong interactors Raf and Ras used in positive control samples (Fig. 2B). A weaker, but still positive β-galactosidase signal (one-third to one-fourth of the Ras-Raf control level; see Fig. 2B) was also observed with AD-EED-394AI and AD-EED-399A4 hybrids, two AD-fused EED mutants defective in MA protein interaction (54). This finding suggested that the IN-binding region in EED differed from the MA-interacting site, mapped to residues 294 to 309 (54) (see also the Table 2 footnotes) but that mutations in the MA-binding domain had some negative effect on the binding of EED to IN in yeast cells. The possibility that EED could have activated transcription of the reporter gene independently of a bona fide interaction with IN-BD hybrid could be excluded since no β-galactosidase signal over the background was detected with the pair of hybrids AD-EED and BD-Ras (Fig. 2) (54).

Mapping of EED-IN interacting sites by phage biopanning. When phages are panned on immobilized EED protein and specific ligand-elution is performed with an excess of affinity-purified IN, the phagotopes isolated would theoretically be mimotopes of peptide motifs of IN, since IN acted as a competitor of phages bound to IN-binding sites on EED (36, 37, 39, 54). Two phage libraries were used—one displaying random hexapeptides and the other displaying random dodecapeptides—on the basis that longer peptides could adopt a conformational structure that would better mimic that of protein interacting sites. About one-third of the phagotopes recovered from both libraries (15 of 50) could be grouped according to recurrent peptide motifs that showed some homology with the C-terminal sequence of IN overlapping tryptophan-235, within residues 212 to 264 (Table 1). For example, motif VLPPK, homologous to 259-VVPRRK in IN, was found several times. However, we observed a high level of degeneration and scatter of all of the phagotopes isolated, suggesting that the EED-binding region in IN had a high degree of three-dimensional organization and/or was constituted of discontinuous epitopes.

Reverse biopanning experiments were then performed to obtain mimotopes of the IN-binding site(s) in EED. The 6-mer library was panned on immobilized IN, and specific ligand elution was performed with an excess of affinity-purified, His-tagged EED-441-H6 protein as the specific competitor for IN-bound phages. The most represented group of phages (14 phages out of 24 independent clones isolated) showed homology with hydrophobic and aromatic motifs within residues 96

TABLE 1. Mimotopes of IN in phages eluted from EED[a]

Library	Phagotope sequence[b]	No. of independent phages isolated	Homologous motif in IN
16-mer	WSNIVV	1	243-WKGEGAVV-250
	EVGPGW	1	229-DSRDPLW-235
	AQNFGQ	1	220-IQNFR-224
	LQTFRQ	1	220-IQNFR-224
12-mer	VLPPKPMRQPVA	3	259-VVPRRK-264
	GIQVANPPRLYG	2	257-IKVVPR-262
	TTGLPLWSFNPS	1	233-PLW-235
	SPWRLPTPLT	1	232-DPLWKGP-238
	QLPFKLGPARID	1	232-DPLWKGPAKL-241
	SHPWNAQRELSV	1	230-SRDPLWK-236
	FSHELSWKPRKA	1	234-LWKGPAKL-241
	VPTNVQLQTPRS	1	212-ELQKQIT-218

[a] Peptide motifs in EED-bound phagotopes showing some homology with the IN sequence are underlined. Note that in a few phages, e.g., SPWRLPTPLT, the phagotope is sometimes shorter than the expected 12-mer.

[b] The amino acid sequence of the HIV-1-BRU IN protein is shown below. The N-terminal domain is made up of the first 50 residues; the C-terminal domain is made up of last 88 residues. The residues involved in the N-terminal zinc finger-like domain are in boldface, the catalytic triad D, D, and E in the core domain is in boldface italics, and the putative region of EED binding (residues 212 to 264) is underlined.

FLDGIDKAQD E**H**EKY**H**SNWR AMASDFNLPP VVAKEIVAS**C** DK**C**QLKGEAM 50
HGQVDCSPGI WQL***D***CTHLEG KVILVAVHVA SGYIEAEVIP AETGQETAYF 100
LLKLAGRWPV KTIHT***D***NGSN FTSTTVKAAC WWAGIKQEFG IPYNPQSQGV 150
V***E***SMNKELKK IIGQVRDQAE HLKTAVQMAV FIHNFKRKGG IGGYSAGERI 200
VDIIATDIQT KELQKQITKI QNFRVYYRDS RDPLWKGPAK LLWKGEGAVV 250
IQDNSDIKVV PRRKAKIIRD YGKQMAGDDC VASRQDED-(288)

to 104, and the other group (4 phages) showed homology with hydrophobic and aromatic motifs within residues 224 to 232 (Table 2). These two putative IN-binding regions were located in the N-terminal moiety of EED and apparently did not overlap with the MA-binding site at positions 294 to 309, which confirmed the results of our two-hybrid assays in yeast (Fig. 2).

EED-IN interaction in vitro analyzed by mutagenesis and pull-down assays. Samples of bacterial cell lysates containing various forms of GST-IN fusion protein (Fig. 3a) were incubated with EED-441-H6 protein, and the resulting complexes were isolated on a glutathione-agarose affinity gel. As shown in Fig. 3b, the binding of full-length WT IN to EED in vitro confirmed the data from our yeast two-hybrid assays and implied that IN and EED proteins could directly interact with each other, without any requirement for a third partner provided by the yeast cell. The possibility that some nucleic acid or protein bridge could link IN and EED in this assay was ruled out on the basis of the following experimental arguments. (i) IN interacted with EED in vitro not only in crude bacterial lysates but also as two affinity-purified recombinant proteins. (ii) In all cases, the bacterial cell lysates from which each protein was recovered were first treated with a broad-spectrum endonuclease from *S. marcescens* (Benzonase; Sigma) that is specific for both single- and double-stranded RNA and DNA substrates. (iii) UV spectrum analyses performed on EED and IN recombinant proteins revealed no detectable nucleic acid contamination, as shown by A280/A260 ratios consistently found to be greater than 1.9.

In order to map the EED-binding region(s) in IN, eight individual deletions scanning the N- and C-terminal structural domains of IN and a double mutant mimicking the IN central core (56) were generated in GST-tagged IN protein (Fig. 1Ba), and the EED-binding capacity of these mutants was evaluated in pull-down assays. Deletions in the N-terminal domain of IN had no negative effect on its binding to EED, and even a slight enhancing effect was observed (Fig. 3b, compare clones 1-288 and N-81), implying that the presence of the N-terminal domain negatively influenced the apparent affinity of IN for EED in vitro. The C-terminal deletion mutant GST-IN-C-273 bound to EED at WT levels, whereas further deletion of residues 273 to 202, as in mutant C-201, reduced the binding to background levels. Likewise, the double-mutant D58-201, which represented the IN core domain (80), bound to EED to insignificant levels (Fig. 3b). The C-terminal region from residues 202 to 273 included the two overlapping sequences from positions 220 to 250 and positions 212 to 264 defined by our biopanning data (Table 1), and this finding confirmed that the C-terminal domain of IN was essential for the IN–EED interaction in vitro.

Since the most represented phagotope retained on immobilized IN corresponded to the sequence 99-VQFNWH-104 in EED (Table 2), a nonconserved mutation in three prominent amino acid residues of this motif was constructed: the bulky tripeptide motif WHS at position 103 to 105 was replaced by a stretch of three alanine residues to generate the EED-103A3 mutant (see Fig. 1Bb). Since this mutation could alter the immunoreactivity of the resulting EED mutant protein, the EED-103A3 mutant was assayed for IN binding as the fusion protein GST-EED-103A3, in comparison with its GST-EED WT counterpart. H6-IN-WT was used as the bait, Ni^{2+}-agarose gel as the trap, and EED proteins were detected by their GST tag by using anti-GST antibodies. EED-103A3 mutant

TABLE 2. Mimotopes of EED in phages eluted from IN[a]

Group	Phagotope sequence[b]	No. of independent phages isolated	Homologous motif in EED
I	VAEWHG	5	99-VQFNWH-104
	FFGLTK	3	96-LFGV-99
	FGQVWS	2	96-LFGVQFNWHS-105
	GANWPS	2	102-NWHS-105
	QGWFWL	1	100-QFNW-103
	MFEVEF	1	96-LFGVQF-101
II	ATVLYG	1	224-TLVAIFG-230
	VRYGP-	1	226-VAIFG-230
	AIAYIG	1	227-AIFGG-231
	ALFLVV	1	227-AIFGGV-232

[a] Peptide motifs in IN-bound phagotopes showing homology with the EED sequence are underlined.

[b] The amino acid sequence of the human EED WT protein is shown below. The seven putative WD repeats are underlined. The N-terminal domain within residues 31 to 63 shows some sequence homology with consensus PEST motifs.

MSEREVSTAP AGTDMPAAKK QKLSSDENSN PDLSGDENDD AVSIESGTNT
ERPDTPTNTP NAPGRKSWGK GKWKSKKCKY 80
SFKCVNSLKE DHNOPLFGVO FNWHSKEGDP LVFATVGSNR VTLYECHSQG
EIRLLQSYVD ADADENFYTC AWTYDSNTSH 160
PLLAVAGSRG IIRIINPITM QCIKHYVGHG NAINELKFHP RDPNLLLSVS
KDHALRLWNI QTDTLVAIFG GVEGHRDEVL 240
SADYDLLGEK IMSCGMDHSL KLWRIYSKRM MNAIKESYDY NPNKTNRPFI
SQKIHFPDFS TRDIHRNYVD CVRWLGDLIL 320
SKSCENAIVC WKPGKMQDDI DKIKPSESNV TILGRFDYSO CDIWYMRFSM
DFWOKMLALG NOVGKLYVW DLEVEDPHKAK 400
CTTLTHHKCG AAIROTSFSR DSSILIAVCD DASIWRWDRL R-(441).

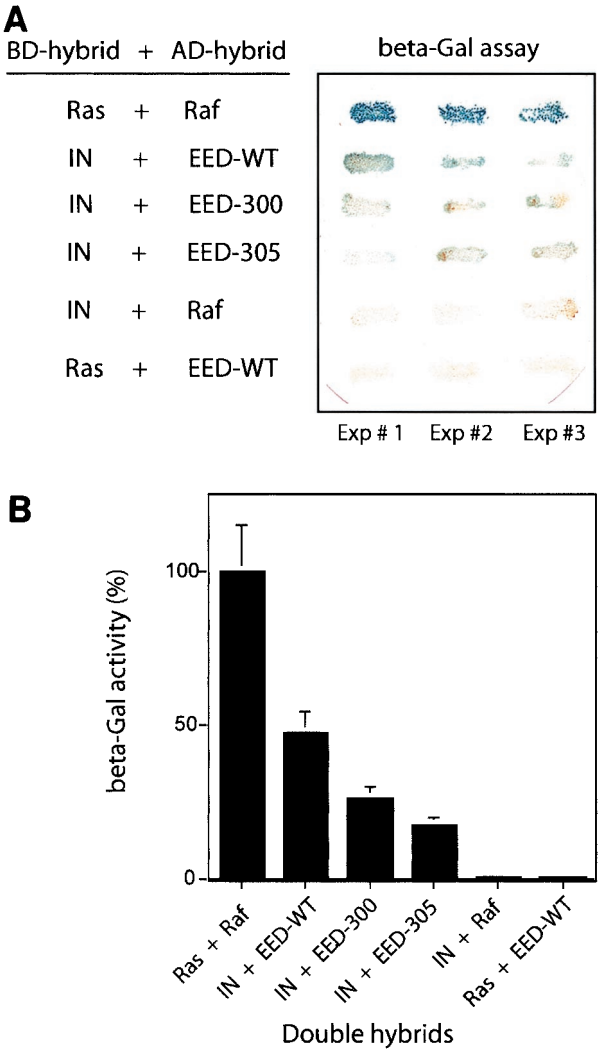

FIG. 2. Interaction of EED and HIV-1 IN in vivo. (A) The affinity of EED (WT or mutants EED-300 and EED-305) for IN was analyzed in yeast by using a two-hybrid assay. IN (or Ras) was cloned in fusion with LexA protein (BD hybrid), and EED (or Raf) was cloned in fusion with the Gal4 activation domain (AD hybrid). The β-galactosidase activity of yeast transformants plated on medium without histidine and replica plated on Whatman filters is shown. The results of three independent experiments are shown. Growth in the absence of His and blue color in the β-Gal assay are indicative of interaction between hybrid proteins in yeast cells. Positive controls involved BD-Ras and AD-Raf hybrids as strong interactors, and negative controls consisted of BD-IN and AD-Raf and of BD-Ras and AD-EED hybrids, respectively. (B) Quantification of β-galactosidase activity in yeast transformants harboring EED and IN hybrids is expressed as the percentage of the BD-Ras plus AD-Raf activity. beta-Gal, β-galactosidase.

was still capable of binding to IN, although with a lower efficiency (two- to threefold; Fig. 3d and e). This suggested that at least one of the IN-binding sites mapped to residues 103 to 105 in EED but that additional IN contact sites could also be present in other domains of EED, as suggested by our phage biopanning (Table 2).

One of the striking features of *Pc*-G gene *eed* products is their high degree of conservation at the protein level in mammals, implying that all amino acid residues of EED are important for their biological functions (51, 68). Thus, it has been shown that the integrity of the last WD repeat of *Pc*-G proteins is highly critical and that even short deletions at the C terminus are detrimental to their activity (51, 76). Consistent with this, the C-terminal deletion mutant EED-C348 was found to bind to the IN-affinity gel at very low levels (Fig. 3d), indicating that the C-terminal fourth of EED was crucial for its interaction with IN, directly or indirectly, via EED conformation and structure stabilization.

Influence of EED on HIV-1 IN activity in vitro. The enzymatic activity of IN was assayed in reactions of DNA integration in vitro in the presence or absence of affinity-purified recombinant EED protein. In IN assays, homologous integration (or autointegration) refers to the integration of one 5′+3′-LTR-containing DNA donor fragment into another (Fig. 4a, band i), whereas heterologous integration (or heterointegration) corresponds to the insertion of one (or more) 5′+3′-LTR-containing fragment(s) into one plasmid target (9). In the absence of EED, several discrete bands of heterointegration products were usually observed: a major band (Fig. 4a, band iii) corresponded to single-tagged circles, resulting from one single integration event per plasmid target, mediated by one LTR (one-ended integration) (10); faster-migrating minor band(s) represented concerted integration events involving two LTRs (Fig. 4a, band ii) and resulting from the insertion of two donors into one target DNA molecule with subsequent linearization (two one-ended concerted integration) and, more rarely, from the two-ended concerted integration of a single donor fragment into target DNA (10). When IN reactions were performed under conditions in which the major band of single-tagged circles (band iii) was the only detectable signal (Fig. 4a, control lane 1), the addition of WT EED provoked an increase in the intensity of autointegration products (band i) and heterointegration products corresponding to single-tagged circles (band iii) (Fig. 4a). The effect became detectable for EED/IN ratios over 2:1 and seemed to occur in a dose-dependent manner, with a twofold augmentation obtained at a ratio of EED to IN of 8:1 (Fig. 4c). However, a 20- to 30-fold augmentation of the putative two one-ended concerted integration products (band ii) was observed within EED/IN ratios ranging from 4:1 to 8:1 (Fig. 4a and c). The same patterns were observed with affinity-purified, WT EED-441-H6 and GST-EED-441, the latter being cleaved off the GST domain. No detectable enhancing effect was observed with corresponding chromatographic fractions from mock-expressing bacterial cells (not shown) or with the deletion mutant protein EED-C348, which provoked a slight and probably nonspecific negative effect at high concentrations (Fig. 4b). This pattern confirmed the interaction between EED and IN proteins in vitro, with a secondary influence on the enzymatic activity of IN.

In situ analysis of IN, EED, and MA proteins in HIV-1-infected cells. Human epithelial HeLa $CD4^+$ cells (P4P56 cells) (52) and lymphoid MT4 cells were infected with BRU-FlagWT, a subclone of $HIV\text{-}1_{BRU}$ expressing a Flag-tagged IN (53). Negative control samples consisted of mock-infected cells or cells incubated with BRU-FlagΔEnv, a noninfectious *env*-deleted mutant used as control for nonspecific HIV-cell interaction. Cells were harvested at 1.5, 6, or 24 h p.i. and processed

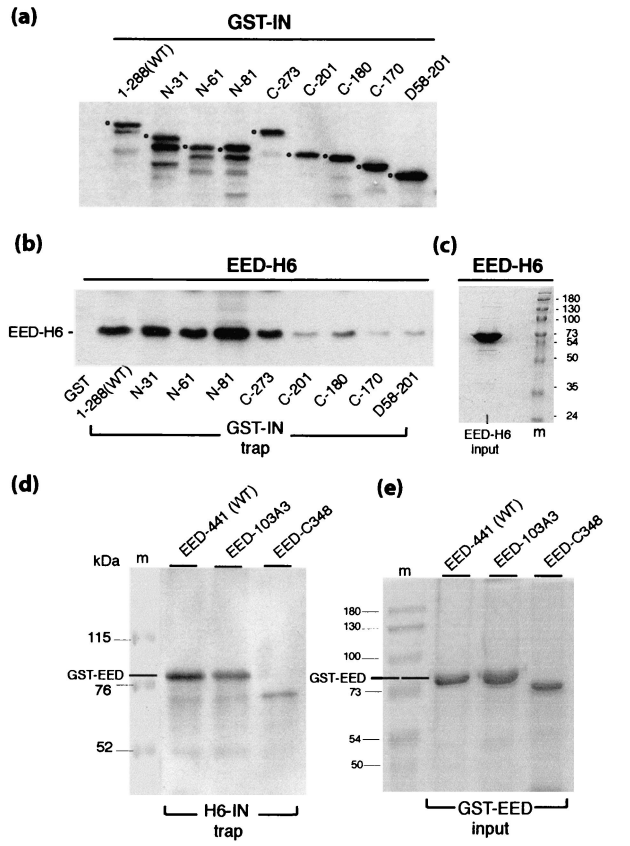

FIG. 3. Interaction of EED and HIV-1 IN in vitro. The affinity between EED and IN and their respective mutants was analyzed by GST and histidine pull-down assays with glutathione-agarose (a to c) and Ni^{2+}-NTA-agarose (d and e) as affinity gels. In panels a to c, aliquots of GST-fused full-length IN (i.e., positions 1 to 288), N-terminal (N), C-terminal (C), and double-deletion (D) mutants, as displayed in panel a, were immobilized on a glutathione-agarose gel, and the affinity gels were incubated with aliquots of bacterial cell lysates containing 10 μg each of full-length, His-tagged EED (EED-H6). The amount of EED-H6 protein retained on GST-IN-glutathione-agarose gel was then evaluated by SDS-PAGE and immunodetection on a blot with anti-His tag MAb as shown in panel b. In panel c is shown EED-H6 input (10-μg protein load; Coomassie blue staining). Note that in panel a, the pattern of anti-GST reacting bands is highly suggestive of a major proteolytic cleavage site located in the C-terminal domain of IN, within region 288-273: a prominent lower band migrating with a constant apparent molecular mass ~2 kDa lower than that of the original GST-IN gene products (marked by solid dots) is visible in samples of full-length and N-deleted forms of GST-IN, whereas this band is absent from the C-truncated or double-truncated GST-IN clones. In panels d and e, the GST-fused, full-length EED, point mutant EED-103A3 and C-terminal deletion mutant EED-C348 were incubated with aliquots of His-tagged IN (H6-IN) adsorbed onto an Ni^{2+}-agarose gel, and the amount of GST-EED protein retained on the H6-IN-Ni^{2+}-agarose gel was determined by SDS-PAGE and immunoblotting with anti-GST polyclonal antibody (panel d). (e) GST-EED protein input (2-μg protein load per well; Coomassie blue staining).

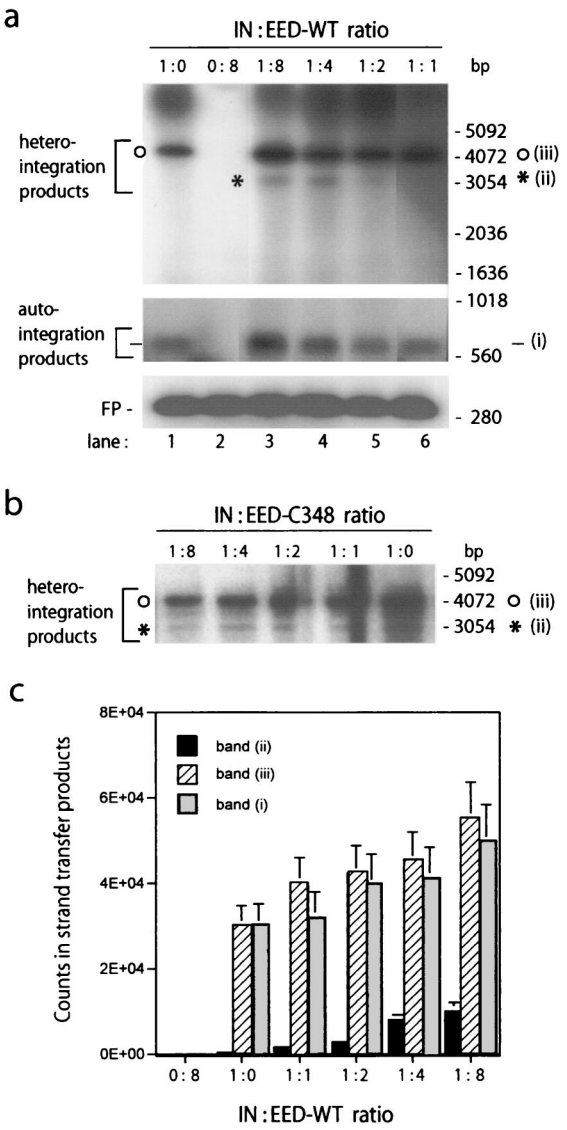

FIG. 4. Effect of EED WT (a and c) and deletion mutant EED-C348 (b) on IN-mediated integration reaction in vitro. The respective IN/EED stoichiometric ratios are indicated at the tops of panels a and b. Control reactions were performed in the absence of EED (lane 1) or in the absence of IN (lane 2). The positions of autointegration products (band i) and heterologous integration products (bands ii and iii) are indicated by brackets on the left. As inferred from previous studies (10, 31), the minor band (band ii [*]) is likely to represent the product of two one-ended concerted integration followed by linearization, whereas the major band (band iii [○]) represents single-tagged target circles. (b) Integration reaction performed in the presence of EED-C348 mutant. Only heterointegration products are shown. (c) Quantification of counts recovered from auto- and heterointegration products of IN reactions performed in the presence of EED-WT (mean of three experiments ± the standard deviation).

for EM and IEM. For IEM analysis, cell specimens were reacted with monoclonal anti-Flag(IN), polyclonal anti-EED, and monoclonal anti-MA MAbs and, occasionally, with anti-CA monoclonal or anti-MA polyclonal antibodies, as indicated. Antibodies were used in single-, double-, or triple-immunolabeling reactions with their corresponding complementary gold-tagged anti-IgG antibody.

At 1.5 h p.i. in mock-infected or BRU-FlagΔEnv-reacted cells, the cytoplasm and nucleus were poorly labeled with anti-MA, anti-CA, and anti-Flag(IN) antibodies, and the immunolabeling corresponded to background reactivity (not shown). In

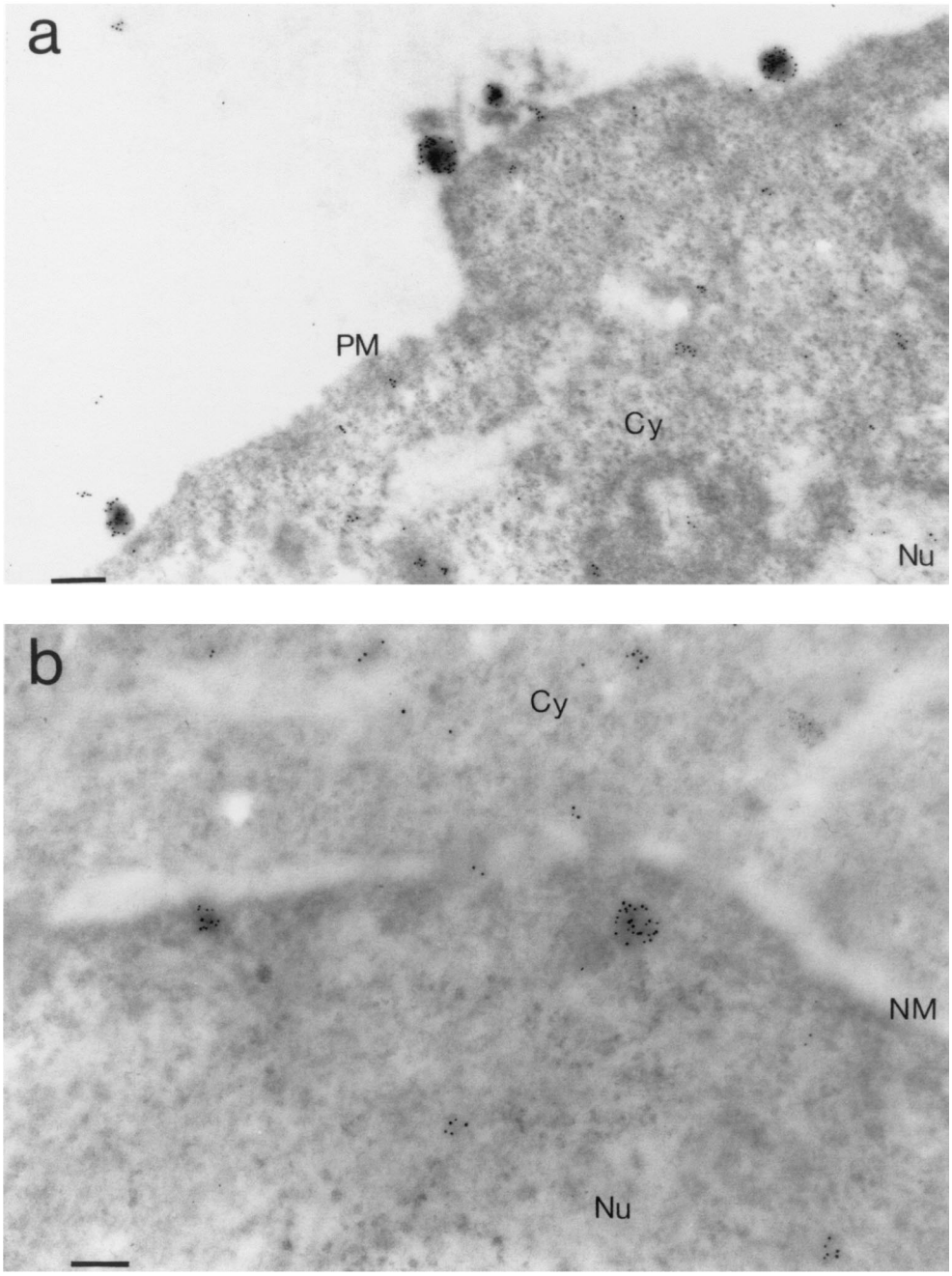

FIG. 5. IEM analysis of human MT4 (a) and HeLa-CD4$^+$ (P4P56) (b) cells infected with Flag-tagged IN-containing HIV-1 (BRU-FlagWT; multiplicity of infection of 1,000 virions/cell) obtained at 1.5 h p.i. In panel a, MA and CA proteins were detected by a mix of anti-MA and anti-CA MAbs, followed by 10-nm-colloidal-gold-tagged anti-mouse IgG antibody. The immunogold-labeled globular structures bound to the cell surface had diameters compatible to those of HIV-1 virions (110 to 130 nm). In P4P56 cells (panel b), the Flag-tagged IN protein was detected by using anti-FLAG MAb (M2), followed by 10-nm-colloidal-gold-tagged anti-mouse IgG antibody. Note that the two gold-labeled globular structures that were 60 to 80 nm in diameter visible in the nucleus in the vicinity of the nuclear membrane had dimensions compatible with those of the PIC. PM, plasma membrane; C, cytoplasm; N, nucleus; NM, nuclear membrane; PM, plasma membrane. Bars: 166 nm (a), 100 nm (b).

BRU-FlagWT-infected cells, however, virus particles were visible in numbers at the cell surface as roughly spherical structures of 120 to 140 nm in diameter that were double labeled with anti-MA and anti-CA antibodies (Fig. 5a). These plasma membrane-associated particles were no longer seen at later times, i.e., at 6 and 24 h p.i.. Within the cells, anti-Flag(IN) antibody-labeled globular structures that were 60 to 80 nm in diameter were visible in significant numbers in the nucleoplasm and frequently seen in the vicinity of nuclear pores (Fig. 5b). Their immunoreactivities and sizes were compatible with those of PICs, which have been reported to be ca. 56 nm in average diameter (49). At 1.5 h p.i., EED labeling was found to

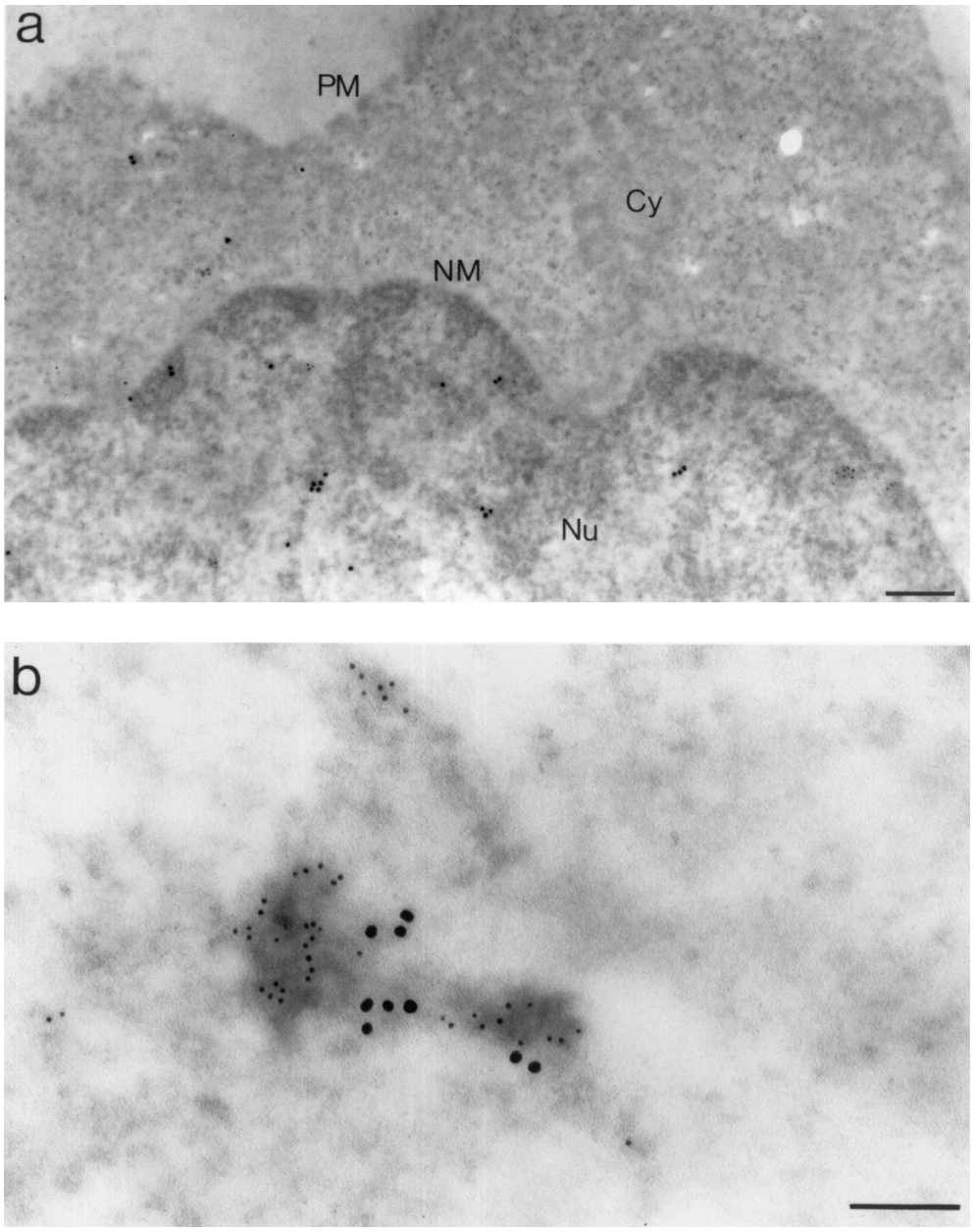

FIG. 6. In situ analysis by IEM of EED and MA proteins in HIV-1-infected MT4 cells taken at 6 h p.i. (a) Mock-infected cells; (b) BRU-FlagWT-infected cells. Cell sections were simultaneously labeled with rabbit anti-EED, detected by using a 10-nm-colloidal-gold-conjugated anti-rabbit IgG antibody, and with anti-MA MAb, detected by a 5-nm-colloidal-gold-conjugated anti-mouse IgG antibody. In panel a, a general view of the cell is shown. In panel b, an area of the nucleoplasm is presented, showing colocalization of 5-nm (MA) and 10-nm (EED) gold grains, associated with electron-dense material. Cy, cytoplasm; Nu, nucleus; PM, plasma membrane; NM, nuclear membrane. Bars: 200 nm (a), 100 nm (b).

be evenly distributed between the cytoplasm and the nucleus and randomly dispersed in both compartments, with no apparent difference between control cells, mock-infected cells, and BRU-FlagΔEnv-treated cells (IEM images not shown; refer to data in Fig. 10a and b).

Double labelings of MT4 and P4P56 cells were then performed to detect a possible colocalization of IN, EED, and MA, pairwise, in the cytoplasm or nucleus at later times p.i. In control cells (mock-infected or BRU-FlagΔEnv-treated cells), double immunolabeling with anti-EED (revealed by 10-nm-gold-tagged conjugate) and anti-IN (5-nm gold grains) or with anti-EED (10-nm gold grains) and anti-MA (5-nm gold grains), respectively, showed that grains of both diameters were randomly distributed in the cytoplasm and nucleoplasm, with no indication of a preferred localization or colocalization at 6 and 24 h p.i. (Fig. 6a and 7a).

The results were different in BRU-FlagWT-infected cells (Fig. 6b). Many patches of electron-dense material were double labeled with anti-MA and anti-EED antibodies in the nucleus of infected cells taken at 6 h p.i. This finding confirmed

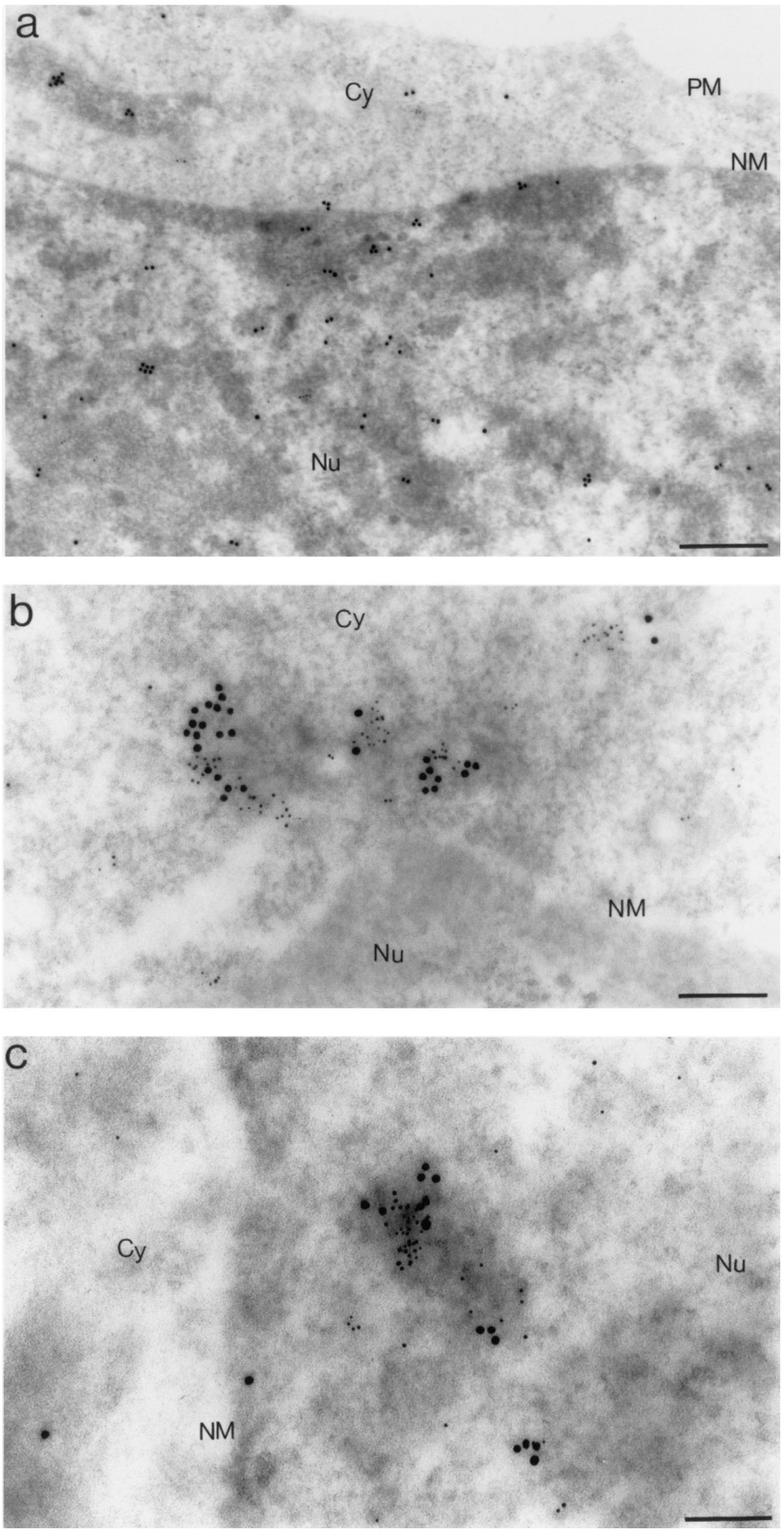

FIG. 7. In situ analysis by IEM of EED and IN proteins in HIV-1-infected human cells at 6 h p.i. Mock-infected MT4 cells (a) and BRU-FlagWT-infected MT4 cells (b) and HeLa-CD4$^+$ cells (P4P56) (c) are shown. Cell sections were simultaneously labeled with anti-EED rabbit antibody, detected by using a 10-nm-colloidal-gold-conjugated anti-rabbit IgG antibody, and with anti-Flag(IN) MAb (M2), detected by using a 5-nm-colloidal-gold-conjugated anti-mouse IgG antibody. Panel a presents a general view of the cell section. Panels b and c show enlargements of sections of nuclear membrane with flanking areas of nucleoplasm and cytoplasm. Cy, cytoplasm; Nu, nucleus; PM, plasma membrane; NM, nuclear membrane. Bars: 333 nm (a), 142 nm (b), 125 nm (c).

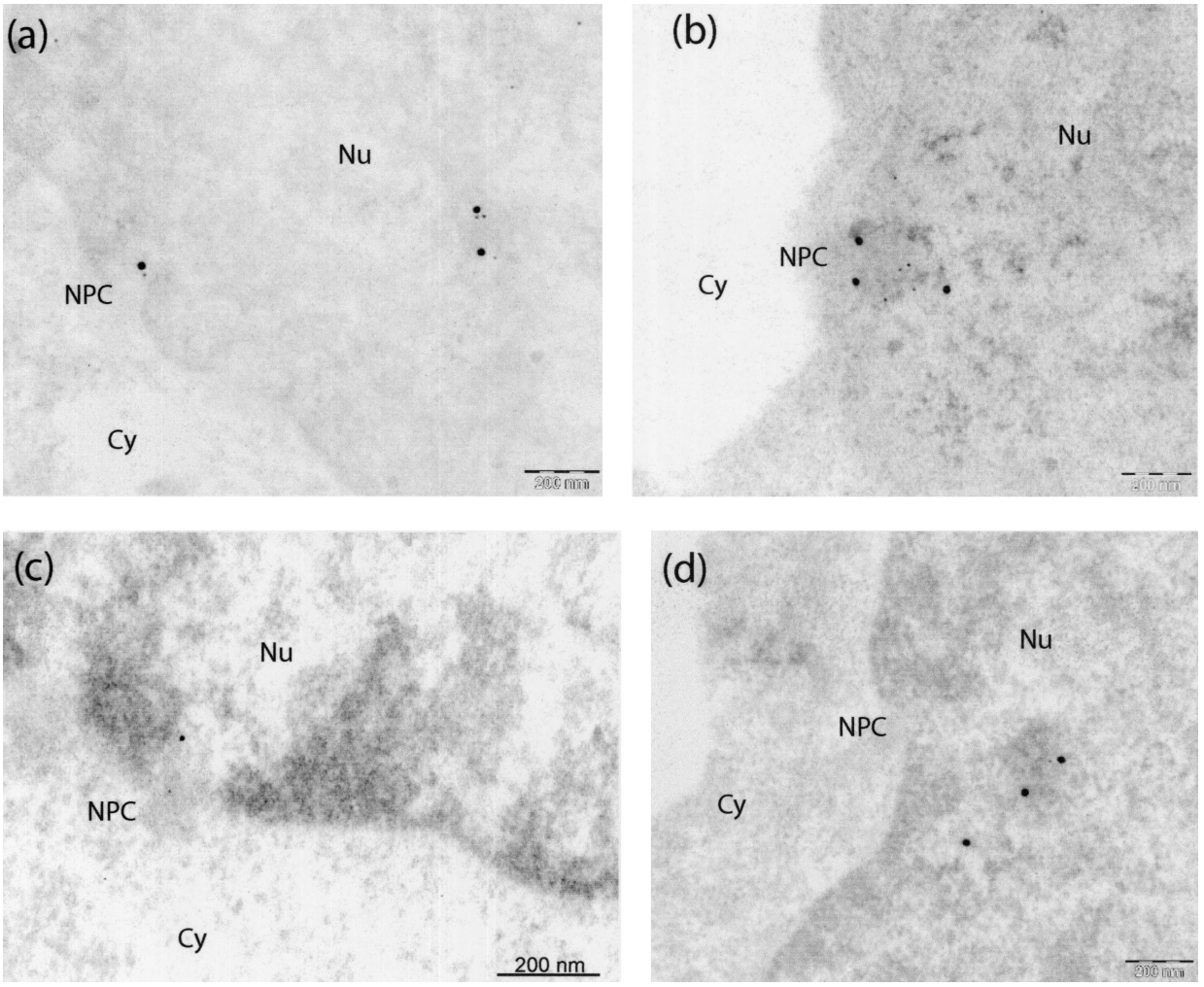

FIG. 8. IEM analysis of colocalization of EED and IN proteins at or near the nuclear pores of BRU-FlagWT-infected MT4 cells obtained at 6 h p.i. The different panels present various areas of cell sections showing nucleoplasm and nuclear pores. Specimens were labeled with rabbit anti-EED, detected by using a 20-nm-colloidal-gold-conjugated anti-rabbit IgG antibody, and anti-Flag(IN) MAb, detected by using a 5-nm-colloidal-gold-conjugated anti-mouse IgG antibody. Cy, cytoplasm; Nu, nucleus; NPC, nuclear pore complex. Bars: 200 nm.

the colocalization of EED and MA proteins already observed in recombinant protein coexpressing insect and human cells (54). Likewise, a pattern of colocalization was observed for IN and EED in BRU-FlagWT-infected MT4 (Fig. 7b) and P4P56 (Fig. 7c) cells taken at 6 h p.i. and double-immunolabeled with anti-IN and anti-EED antibodies. Colocalizations of IN and EED were mainly observed in the nucleus (Fig. 7c) but were also observed in the cytoplasm in close vicinity to the nuclear membrane (Fig. 7b). IN-EED colocalizations were frequently seen at or near the nuclear pores (Fig. 8). In most of these observations, the clusters of EED- and IN-bound grains were found to be associated with electron-dense material in the nucleoplasm or at the nuclear pores (Fig. 6 to 8). IN-EED colocalizations were no longer observed at 24 h p.i.

In order to detect a possible colocalization of the three proteins IN, EED, and MA, triple-immunolabeling experiments were also performed with anti-EED (revealed by 20-nm colloidal gold grain), anti-MA (10-nm colloidal gold grain), and anti-IN (5-nm colloidal gold grain) antibodies on sections of BRU-FlagWT-infected MT4 and P4P56 cells. Many clusters of gold grains of the three different diameters were found in nuclei at 6 h p.i. (Fig. 9). Such triple colocalizations were never observed in control samples, mock-infected cells, and BRU-FlagΔEnv-treated cells. Our IEM data therefore suggested that IN, MA, and EED proteins could form ternary complexes and/or participate together in higher-order complexes in vivo within the nucleus of HIV-1-infected cells at early times p.i.

Quantitative IEM analysis of the cellular distribution and colocalization of IN, EED, and MA proteins in HIV-1-infected cells. To further analyze the distribution of EED, IN, and MA proteins in the cellular compartments in a semiquantitative and kinetic manner, sections of control or HIV-1-infected P4P56 or MT4 cells were separately reacted with rabbit anti-EED, anti-IN and anti-MA IgG, followed by 10-nm-gold conjugated anti-rabbit IgG antibody in single immunogold labeling experiments. Gold grains were counted by using EM in several sections of independent cells taken at time intervals during HIV-1 infection. At least 400 grains were counted on 20 dif-

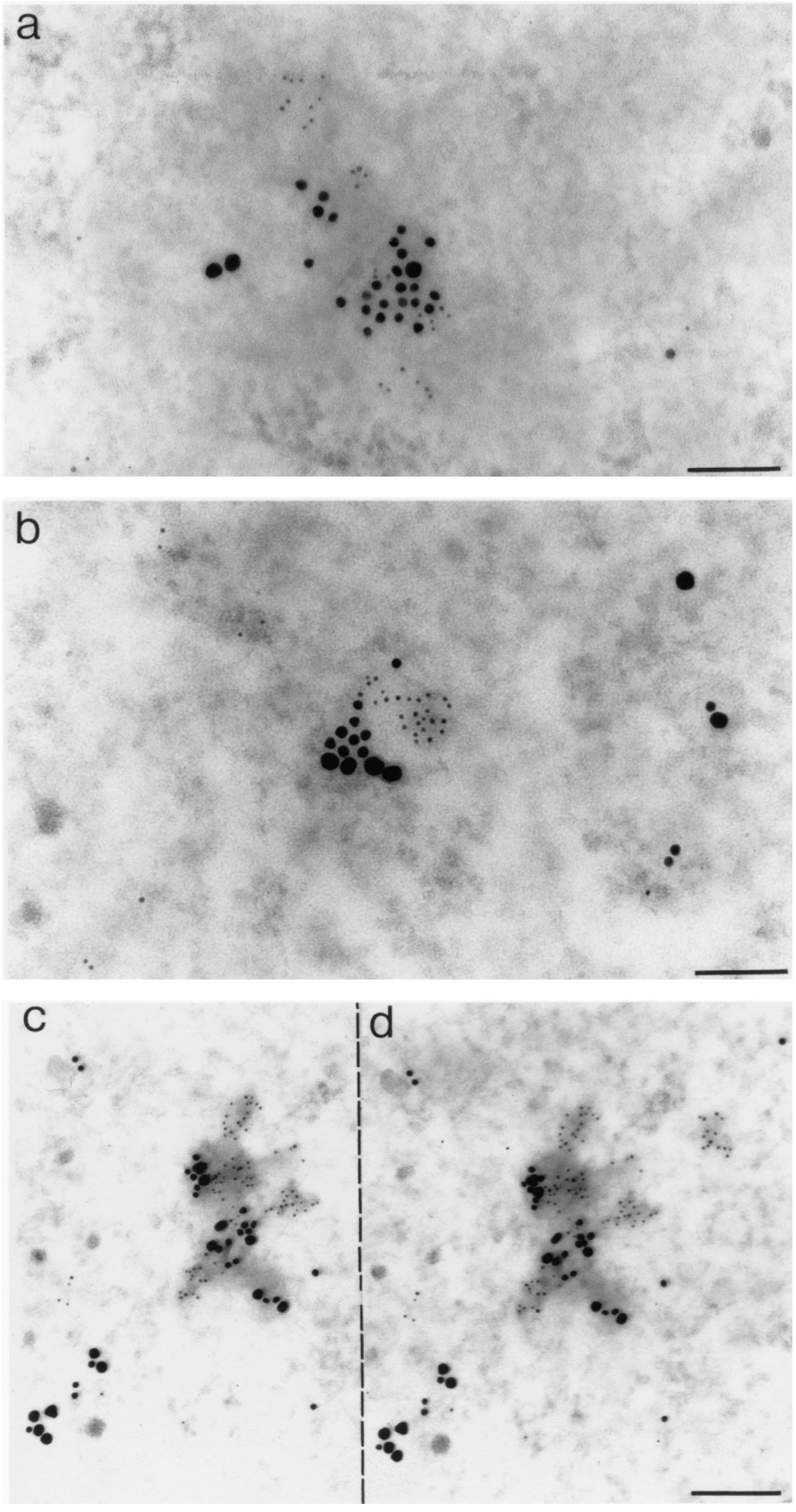
a
b
c
d

ferent cell sections, and the variations of the density of grains (number of grains per unit surface area of cell section) in the cytoplasm (Fig. 10a) and nucleus (Fig. 10b) were compared during the course of infection. Backgound labeling was given by mock-infected cells reacted with the same primary and gold-conjugated secondary antibodies (zero time point).

In HIV-1-infected cells, MA labeling was detected as early as at 1.5 h p.i. in both cytoplasm (Fig. 10a) and nucleus (Fig. 10b). The MA signal decreased to background levels at 6 h p.i. in the cytoplasm but was still observed at significant levels in the nucleus until 6 h p.i. In the cytoplasm, the IN labeling was not significantly higher than the background level at any time p.i. (Fig. 10a). In the nucleus however, IN signal was detected at 1.5 h p.i. and reached a maximum level at 6 h p.i., suggesting a higher number, or better accessibility, of IN molecules at this time of the virus cycle (Fig. 10b; see also Fig. 5b). The level of EED labeling remained almost constant throughout the time period in both cytoplasmic and nuclear compartments (Fig. 10a and b). No significant variation and increase over the background labeling was observed in BRU-FlagΔEnv-infected P4P56 or MT4 cells for the three markers, MA, IN, and EED, during the same time period (background line; Fig. 10c).

Colocalization of EED, IN, and MA proteins was also quantitavely evaluated by EM by counting neighboring grains on sections from cells taken at different times p.i. and subjected to triple immunolabeling with specific monoclonal and polyclonal antibodies (see, for example, Fig. 9). This quantitative assay was based on the following principle. The size of an antibody molecule under EM is ca. 15 nm and, in our IEM analyses, primary and secondary gold-labeled antibody molecules were used. Thus, if one antibody is labeled with a 10-nm gold grain and the other one is labeled with a 20-nm grain and if both gold conjugations occurred at their respective Fc domains, the two gold grains that are 90 nm apart (15 + 15 + 10 + 15 + 15 + 20 nm) might theoretically mark two adjacent epitopes carried by the same protein molecule or, alternatively, two epitopes belonging to two neighboring molecules. Since epitopes on interacting proteins could lie at a certain distance from each other, one could reasonably consider that immunogold grains that are seen within a distance range of 100 to 120 nm would mark molecules that colocalize in the same cell compartment.

Using this quantitative method, we observed no significant colocalization of grains marking EED, MA, and IN in the cytoplasm and nucleus of mock-infected cells or in cells incubated with BRU-FlagΔEnv (Fig. 10c). Likewise, colocalization of gold grains marking IN, MA, and EED was rarely observed in the cytoplasm of BRU-FlagWT-infected cells at early times p.i. (e.g., 1.5 h p.i.), and no statistical analysis could be performed (results not shown). The results were different for the nuclei of BRU-FlagWT-infected cells, which showed clusters of double and even triple colocalizations with a significant frequency (Fig. 10c). An average value of three colocalization events per square micrometer of nucleoplasm area was found for the pair IN-MA at 1.5 h p.i., but no other pairwise colocalization (IN-EED or MA-EED) was found in significant numbers. At later times, no more colocalization of IN and MA was observed. At 6 h p.i., a mean value of two colocalization events per square micrometer was found for IN and EED, and triple colocalization of EED, IN and MA occurred at an average frequency of one event per square micrometer of nucleus section area (Fig. 10c). No detectable double or triple colocalizations were detectable at 24 h p.i. This finding suggested that the time point of 6 h p.i. represented the phase of the virus cycle when significant numbers of EED, IN, and MA molecules were in close vicinity within the nucleus of HIV-1-infected cells. Alternatively, it could mean that the intranuclear microenvironment that allowed for a maximal immunoreactivity and accessibility of the three proteins took place at 6 h p.i.

DISCUSSION

We found here that human EED, a *Pc*-G protein, can interact with HIV-1 IN both in vitro and in vivo in yeast. Using deletion mutagenesis and phage biopanning, we mapped the major EED-binding sites to the C-terminal domain of IN. In vitro, we observed an apparent positive effect of EED on IN-mediated integration reaction. We hypothesize that this effect was indirect: the interaction of EED with IN could promote the oligomerization of IN molecules, which would in turn favor the integration process. In situ analysis of EED and IN cellular localization was performed on HIV-1-infected human epithelial (HeLa $CD4^+$) or lymphoid (MT4) cells by using IEM and differential immunogold labeling. We found that EED and IN colocalized within the nucleus of HIV-infected cells, a phenomenon that was mainly observed at early times p.i. (1.5 to 6 h). Triple-immunolabeling experiments showed that the MA protein, another viral protein partner of EED (54), was also detected in significantly frequent associations with both EED and IN proteins in the nucleus at early times p.i., suggesting the occurrence of ternary complexes involving EED, MA, and IN. Although the role of EED protein in the HIV-1 life cycle is not known, our data suggest that EED could be involved in some cellular function(s) necessary for and/or induced by early steps of the virus-host cell interaction. The fact that we never observed any cellular colocalization of EED, IN, and MA in cells infected with HIV-1 in the presence of virus inhibitor AZT

FIG. 9. In situ analysis by IEM of IN, EED, and MA proteins by using triple immunogold labeling of EM sections of BRU-FlagWT-infected human cells taken at 6 h p.i. (a) MT4 cell nucleoplasm; (b to d) HeLa $CD4^+$ cell (P4P56) nucleoplasm. In a first step, one side of the grid carrying the cell pellet section was simultaneously reacted with mouse anti-Flag(IN) MAb and rabbit anti-MA antibody and then with a mix of 5-nm-gold-conjugated anti-mouse IgG antibody and 10-nm-gold-conjugated anti-rabbit IgG antibody. In a second step, the other side of the grid was incubated with rabbit anti-EED antibody, detected by using a 20-nm-gold-conjugated anti-rabbit IgG antibody. (c and d) Stereoscopic view of a portion of P4P56 cell nucleus, taken upon tilting the microscope goniometer, showing clusters of grains 5 nm (IN), 10 nm (MA), and 20 nm (EED) in diameter, in association with electron-dense nucleoplasmic material. By using stereoscopic glasses and aiming at the dotted line separating panels c and d, one can see that the 20-nm gold grains belong to a plane different from that of the 5- and 10-nm grains and that there was no cross-labeling between anti-MA (top side of the specimen) and anti-EED primary IgG (bottom side of the specimen) by the secondary anti-IgG antibody. Bars: 100 nm (a and b), 166 nm (c and d).

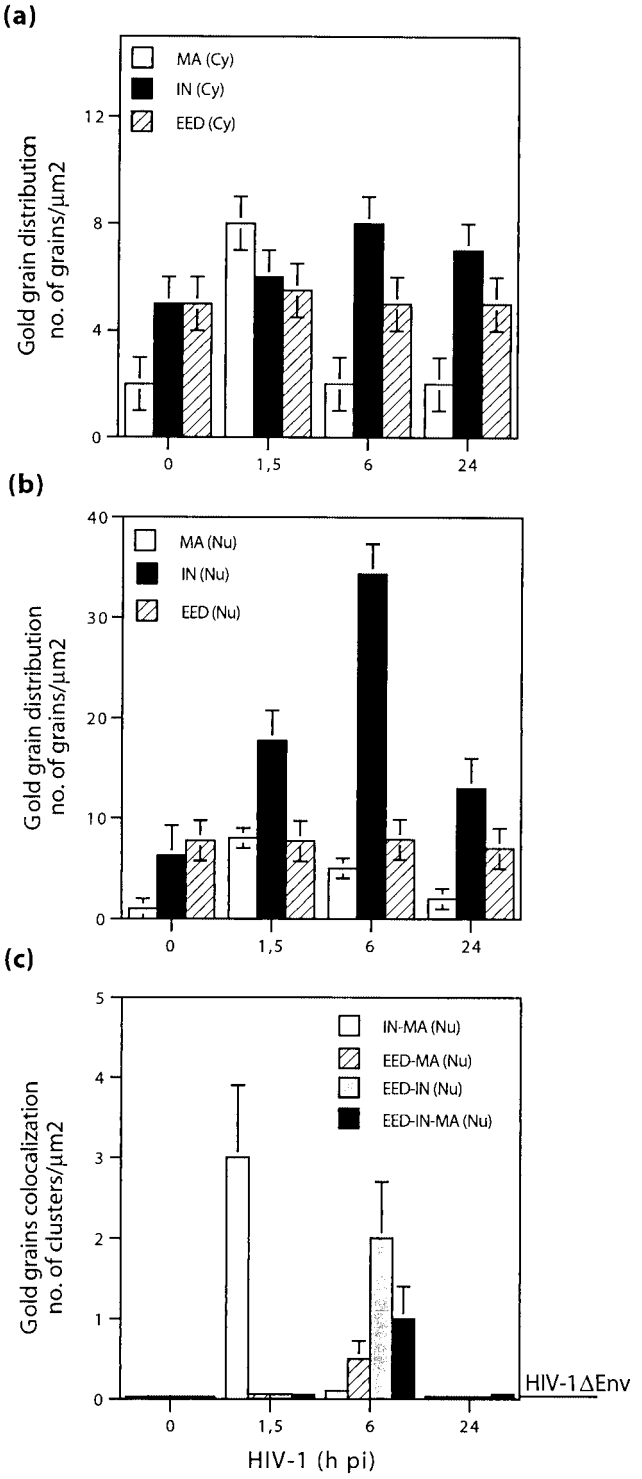

FIG. 10. Quantitative image analysis of intracellular distribution (a and b) and nuclear colocalization (c) of EED, MA, and IN proteins in HIV-1-infected MT4 cells. Cells infected with BRU-FlagWT, or its noninfectious, envelope-deleted version BRU-FLAGΔEnv, were harvested at different times p.i. as indicated on the *x* axis. (a) Cytoplasm; (b and c) nucleus. In panels a and b, gold grains were counted on cell sections after single labeling with affinity-purified anti-EED, anti-MA, or anti-IN rabbit antibodies, respectively, followed by 10-nm-gold-tagged anti-rabbit IgG antibody. Background labeling for IN and MA proteins was given by the number of grains per square micrometer on mock-infected cell sections (zero point). In panel c are shown the results of triple-labeling experiments (see, for example, Fig. 9). The baseline on the right corresponds to the data obtained with BRU-FLAGΔEnv (HIV-1ΔEnv).

(data not shown) suggests that the role played by EED in the virus cycle would require the step of proviral DNA synthesis. Since EED is a partner of two viral proteins—MA, which has both structural and functional roles at the early stages of the cycle (23), and IN, which is responsible for proviral integration—one might envisage EED as a possible participant in at least two major retroviral processes: the intracellular transport of incoming virions and/or the proviral integration.

In spite of a number of studies (2, 13, 16, 24–27, 35, 40, 48, 49, 52, 84, 85), the cellular and viral factors that control the reaction and the site(s) of integration of HIV-1 proviral DNA still remain incompletely elucidated. The integration process is better understood at the molecular level for retrotransposons, such as Ty5, which integrates into regions of silent chromatin via yeast proteins Sir (86). Like the Sir proteins in yeast, the products of many *Pc*-G genes are responsible for the maintenance of the silent state of chromatin in upper eukaryotes, likely by recruitment of histone deacetylases (reviewed in reference 55). Thus, the transcriptional repression by EED has been recently reported to involve histone deacetylation (79). Likewise, in murine neurons, EED has been shown to colocalize with histone H1 in transcriptionally inactive domains of perinucleolar heterochromatin (1). The function of *Pc*-G proteins as transcriptional repressors and gene silencers (17, 33, 51, 63, 67, 74) has been attributed in several cases to direct interaction with transcription factors rather than to direct DNA binding (3, 64). For example, EED has been found to bind to YY1, a vertebrate DNA-binding protein (4), and a stable, if only transient, interaction between EED, EZH2 (enhancer of Zeste 2) (70), YY1, and histone deacetylase has been suggested (62). An indirect physical link has therefore been established between EED and the DNA of target chromatin regions via the DNA-binding protein YY1 (62).

In light of the latest results on HIV-1 integration into transcriptionally active regions of the host genome (66, 83), an attractive hypothesis would be that intranuclear interaction occurring between the viral proteins MA and IN on one side and the cellular protein EED on the other side might deregulate silent cellular genes by releasing the binding of EED to YY1 (or other factors involved in the transcription machinery), by modifying the acetylation state of histones, or by both of these processes. This would then activate the integration process of the proviral DNA. However, it is important to note that YY1 is a multifunctional transcription factor which, under certain circumstances, can act as a transcriptional repressor (72).

Alternatively, but not exclusively, there may be a role in the intracellular transport and nuclear translocation of the PIC for EED. As a component of a multifactor transport complex, EED might act as a shuttle protein to convoy the viral PIC to the nucleus via its binding to MA and IN. Only a few cellular proteins have been identified thus far as involved in the transport of HIV-1 PIC. A DNA targeting function has been assigned to the product of the *INI1* gene (40), a cellular inter-

actor of HIV-1 IN that seems to also act in late events in the viral life cycle (84). It has been shown that HIV-1 PIC recruits INI1 and PML proteins within the cytoplasm, and this complex could facilitate the integration via the recruitment of additional cell factors, such as the PML-binding CBP/p300 (78). Interestingly, a protein similar to EED, called WAIT-1 (WD protein associated with integrin cytoplasmic tails-1) (61), has been found to interact with the cytoplasmic domain of the integrin β7 subunits, and a shuttling of WAIT-1/EED between membrane-associated β7 integrins and the nucleus has been suggested (61). The β7 cytoplasmic domain is involved in major integrin functions such as receptor affinity and signaling (15, 46). It is noteworthy that, among the β7 subfamily members, αEβ7 integrin is restricted to a subset of gut-associated T lymphocytes and dendritic cells (61). The frequent occurrence of EED and IN double labeling at nuclear pore complexes, as observed in our IEM study, would support a shuttling function for EED. Further investigations by cell fractionation of HIV-1-infected cells, overexpression versus synthesis inhibition of EED in HIV-infected cells, and isolation of dominant-negative mutants of EED would help elucidate the role(s) of cellular EED protein in HIV-1 infection.

ACKNOWLEDGMENTS

This work was supported by the Agence Nationale de Recherche sur le SIDA (ANRS; AC14-2 "HIV-1 Integrase and Preintegration Complex"). S.V. received an ANRS fellowship, and S.P. received a fellowship from the French ECS Association (Ensemble contre le SIDA).

We are deeply grateful to Simone Peyrol and Isabelle Leparc-Goffart (Centre d'Imagerie de la Faculté de Médecine Laennec) and to Paul Paulet (Centre Régional d'Imagerie Cellulaire de Montpellier) for significant contributions to the EM specimen processing, image digitalization, and photography. We are also grateful to Jean-Claude Cortay for valuable advice on pT7-7 cloning, fast-performance liquid chromatography, and protein purification. We thank Roger Monier, Catherine Dargemont, Robert Vigne, Etienne Decroly, Gilles Quérat, and Corinne Ronfort for fruitful discussions during this study. We are indebted to François Grateau, Hospices Civils de Lyon, for the financing of the MegaView II TEM camera and automatic MT-X ultramicrotome (RMC EM Products Group, Ventana Medical Systems, Inc., Tucson, Ariz.).

REFERENCES

1. **Akhmanova, A., T. Verkerk, A. Langeveld, F. Grosveld, and N. Galijart.** 2000. Characterisation of transcriptionally active and inactive chromatin domains in neurons. J. Cell Sci. **113:**4463–4474.
2. **Bouyac-Bertoia, M., J. D. Dvorin, R. A. Fouchier, Y. Jenkins, B. E. Meyer, L. I. Wu, M. Emerman, and M. H. Malim.** 2001. HIV-1 infection requires a functional integrase NLS. Mol. Cell **7:**1025–1035.
3. **Breilling, A., B. M. Turner, M. E. Bianchi, and V. Orlando.** 2001. General transcription factors bind promoters repressed by *Polycomb* group proteins. Nature **412:**651–655.
4. **Brown, J. L., D. Mucci, M. Whiteley, M. L. Dirksen, and J. A. Kassis.** 1998. The *Drosophila Polycomb* group gene pleiohomeotic encodes a sequence-specific DNA binding protein with homology to the multifunctional mammalian transcription factor YY1. Mol. Cell **7:**1057–1064.
5. **Brown, P. O.** 1997. Integration. Cold Spring Harbor Laboratory Press, Cold Spring Harbor, N.Y.
6. **Bukrinsky, M. I., S. Haggerty, M. P. Dempsey, N. Sharova, A. Adzhubei, L. Spitz, P. Lewis, D. Goldfarb, M. Emerman, and M. Stevenson.** 1993. A nuclear localization signal within HIV-1 matrix protein that governs infection of non-dividing cells. Nature **365:**666–669.
7. **Bukrinsky, M. I., N. Sharova, T. L. McDonald, T. Pushkarskaya, W. G. Tarpley, and M. Stevenson.** 1993. Association of integrase, matrix, and reverse transcriptase antigens of human immunodeficiency virus type 1 with viral nucleic acids following acute infection. Proc. Natl. Acad. Sci. USA **90:**6125–6129.
8. **Carrière, C., B. Gay, N. Chazal, N. Morin, and P. Boulanger.** 1995. Sequence requirement for encapsidation of deletion mutants and chimeras of human immunodeficiency virus type 1 Gag precursor into retrovirus-like particles. J. Virol. **69:**2366–2377.
9. **Carteau, S., S. C. Batson, L. Poljak, J.-F. Mouscadet, H. de Rocquigny, J.-L. Darlix, B. P. Roques, E. Käs, and C. Auclair.** 1997. Human immunodeficiency virus type 1 nucleocapsid protein specifically stimulates Mg^{2+}-dependent DNA integration in vitro. J. Virol. **71:**6225–6229.
10. **Carteau, S., R. J. Gorelick, and F. D. Bushman.** 1999. Coupled integration of human immunodeficiency virus type 1 cDNA ends by purified integrase in vitro: stimulation by the viral nucleocapsid protein. J. Virol. **73:**6670–6679.
11. **Carteau, S., C. Hoffmann, and F. D. Bushman.** 1998. Chromosome structure and human immunodeficiency virus type 1 cDNA integration: centromeric alphoid repeats are a disfavored target. J. Virol. **72:**4005–4014.
12. **Chazal, N., B. Gay, C. Carrière, J. Tournier, and P. Boulanger.** 1995. Human immunodeficiency virus type 1 MAp17 deletion mutants expressed in baculovirus-infected cells: *cis* and *trans* effects on the Gag precursor assembly pathway. J. Virol. **69:**365–375.
13. **Chicurel, M.** 2000. Probing HIV's elusive activities within the host cell. Science **290:**1876–1879.
14. **Cortay, J.-C., D. Nègre, M. Scarabel, T. M. Ramseler, N. B. Vartak, J. Reizer, and A. J. Cozzone.** 1994. In vitro asymmetric binding of the pleiotropic regulatory protein, FruR, to the *ace* operator controlling glyoxylate shunt enzyme synthesis. J. Biol. Chem. **269:**14885–14891.
15. **Crowe, D. T., H. Chiu, S. Fong, and I. L. Weissmann.** 1994. Regulation of the avidity of integrin $\alpha_4\beta_7$ by the β_7 cytoplasmic domain. J. Biol. Chem. **269:**14411–14418.
16. **Cullen, B.** 2001. Journey to the center of the cell. Cell **105:**697–700.
17. **Denisenko, O. N., and K. Bomsztyk.** 1997. The product of the murine homolog of the *Drosophila extra sex combs* gene displays transcriptional repressor activity. Mol. Cell. Biol. **17:**4707–4717.
18. **Dvorin, J. D., P. Bell, G. G. Maul, M. Yamashita, M. Emerman, and M. H. Malim.** 2002. Reassessment of the roles of integrase and the central DNA flap in human immunodeficiency virus type 1 nuclear import. J. Virol. **76:**12087–12096.
19. **Farnet, C. M., and F. D. Bushman.** 1997. HIV-1 cDNA integration: requirement of HMG I(Y) protein for function of preintegration complexes in vitro. Cell **88:**483–492.
20. **Farnet, C. M., and W. A. Haseltine.** 1990. Integration of human immunodeficiency virus type 1 DNA in vitro. Proc. Natl. Acad. Sci. USA **87:**4164–4168.
21. **FitzGerald, D. P., and W. Bender.** 2001. Polycomb group repression reduces DNA accessibility. Mol. Cell. Biol. **21:**6585–6597.
22. **Fouchier, R. A., B. E. Meyer, J. H. Simon, U. Fischer, A. V. Albright, F. Gonzales-Scarano, and M. H. Malim.** 1998. Interaction of the human immunodeficiency virus type 1 Vpr protein with the nuclear pore complex. J. Virol. **72:**6004–6013.
23. **Freed, E. O.** 1998. HIV-1 Gag proteins: diverse functions in the virus life cycle. Virology **251:**1–15.
24. **Gallay, P., T. Hope, D. Chin, and D. Trono.** 1997. HIV-1 infection of nondividing cells through the recognition of integrase by the importin/karyopherin pathway. Proc. Natl. Acad. Sci. USA **94:**9825–9830.
25. **Gallay, P., V. Stitt, C. Mundy, M. Oettinger, and D. Trono.** 1996. Role of the karyopherin pathway in human immunodeficiency virus type 1 nuclear import. J. Virol. **70:**1027–1032.
26. **Gallay, P., S. Swingler, C. Aiken, and D. Trono.** 1995. HIV-1 infection of nondividing cells: C-terminal tyrosine phosphorylation of the viral matrix protein is a key regulator. Cell **80:**379–388.
27. **Gallay, P., S. Swingler, J. Song, F. Bushman, and D. Trono.** 1995. HIV nuclear import is governed by the phosphotyrosine-mediated binding of matrix to the core domain of integrase. Cell **83:**569–576.
28. **Gao, K., R. J. Gorelick, D. G. Johnson, and F. Bushman.** 2003. Cofactors for human immunodeficiency virus type 1 cDNA integration in vitro. J. Virol. **77:**1598–1603.
29. **Gay, B., J. Tournier, N. Chazal, C. Carrière, and P. Boulanger.** 1998. Morphopoietic determinants of HIV-1 GAG particles assembled in baculovirus-infected cells. Virology **247:**160–169.
30. **Goff, S. P.** 2001. Intracellular trafficking of retroviral genomes during the early phase of infection: viral exploitation of cellular pathways. J. Gene Med. **3:**517–528.
31. **Goodarzi, G., G. J. Im, K. Brackmann, and D. Grandgenett.** 1995. Concerted integration of retrovirus-like DNA by human immunodeficiency virus type 1 integrase. J. Virol. **69:**6090–6097.
32. **Guan, K. L., and J. E. Dixon.** 1991. Eukaryotic proteins expressed in *Escherichia coli*: an improved thrombin cleavage and purification procedure of fusion proteins with glutathione *S*-transferase. Anal. Biochem. **192:**262–267.
33. **Gutjarhr, T., E. Frei, S. C., S. Baumgatner, A. H. White, and M. Noll.** 1995. The polycomb-group gene, extra sex combs, encodes a nuclear member of the WD40 repeat family. EMBO J. **14:**4296–4306.
34. **Higuchi, R., B. Krummel, and R. K. Saiki.** 1988. A general method of in vitro preparation and specific mutagenesis of DNA fragments: study of protein and DNA interactions. Nucleic Acids Res. **16:**7351–7367.
35. **Hindmarsh, P., and J. Leis.** 1999. Retroviral DNA integration. Microbiol. Mol. Biol. Rev. **63:**836–843.
36. **Hong, S. S., and P. Boulanger.** 1995. Protein ligands of human adenovirus type 2 outer capsid identified by biopanning of a phage-displayed peptide

library on separate domains of WT and mutant penton capsomers. EMBO J. **14:**4714–4727.
37. **Hong, S. S., L. Karayan, J. Tournier, D. T. Curiel, and P. A. Boulanger.** 1997. Adenovirus type 5 fiber knob binds to MHC class I α2 domain at the surface of human epithelial and B lymphoblastoid cells. EMBO J. **16:**2294–2306.
38. **Horten, R. M., H. D. Hunt, S. N. Ho, J. K. Pullen, and P. L. R.** 1989. Engineering hybrid genes without the use of restrictions enzymes: gene splicing by overlap extension. Gene **77:**61–68.
39. **Huvent, I., S. S. Hong, C. Fournier, B. Gay, J. Tournier, C. Carriere, M. Courcoul, R. Vigne, B. Spire, and P. Boulanger.** 1998. Interaction and coencapsidation of HIV-1 Vif and Gag recombinant proteins. J. Gen. Virol. **79:**1069–1081.
40. **Kalpana, G. V., S. Marmon, W. Wang, G. R. Crabtree, and S. P. Goff.** 1994. Binding and stimulation of HIV-1 integrase by a human homolog of yeast transcription factor SNF5. Science **266:**2002–2006.
41. **Lee, M. S., and R. Craigie.** 1998. A previously unidentified host protein protects retroviral DNA from autointegration. Proc. Natl. Acad. Sci. USA **95:**1528–1533.
42. **Leh, H., P. Brodin, J. Bischerour, E. Deprez, P. Tauc, J.-C. Brochon, E. LeCam, D. Coulaud, C. Auclair, and J.-F. Mouscadet.** 2000. Determinants of Mg^{2+}-dependent activities of recombinant human immunodeficiency virus type 1 integrase. Biochemistry **39:**9285–9294.
43. **Lin, C.-W., and A. Engelman.** 2003. The barrier-to-autointegration factor is a component of functional human immunodeficiency virus type 1 preintegration complexes. J. Virol. **77:**5030–5036.
44. **Lutzke, R. A., and R. H. Plasterk.** 1998. Structure-based mutational analysis of the C-terminal DNA-binding domain of the human immunodeficiency virus type 1 integrase: critical residues for protein oligomerization and DNA binding. J. Virol. 4841–4848.
45. **Maertens, G., P. Cherepanov, W. Pluymers, K. Busschots, E. De Clercq, Z. Debyser, and Y. Engelborghs.** 2003. LEDGF/p75 is essential for nuclear and chromosomal targeting of HIV-1 integrase in human cells. J. Biol. Chem. **278:**372–381.
46. **Manié, S. N., A. Astier, D. Wang, J. S. Phifer, J. Chen, A. I. Lazarovits, C. Morimoto, and A. S. Freedman.** 1996. Stimulation of tyrosine phosphorylation after ligation of β7 and β1 integrins on human B cells. Blood **87:**1855–1861.
47. **Margottin, F., S. P. Bour, H. Durand, L. Selig, S. Benichou, V. Richard, D. Thomas, K. Strebel, and R. Benarous.** 1998. A novel human WD protein, h-beta TrCP, that interacts with HIV-1 Vpu connects CD4 to the ER degradation pathway through an F-box motif. Mol. Cell **1:**565–574.
48. **Miller, M. D., and F. D. Bushman.** 1995. Ini1 for integration? Curr. Biol. **5:**368–370.
49. **Miller, M. D., C. M. Farnet, and F. D. Bushman.** 1997. Human immunodeficiency virus type 1 preintegration complexes: studies of organization and composition. J. Virol. **71:**5382–5390.
50. **Neer, E. J., C. J. Schmidt, R. Nambudripad, and T. F. Smith.** 1994. The ancient regulatory-protein family of WD-repeat proteins. Nature **371:**297–300.
51. **Ng, J., R. Li, K. Morgan, and J. Simon.** 1997. Evolutionary conservation and predicted structure of the *Drosophila* extra sex combs repressor protein. Mol. Cell. Biol. **17:**6663–6672.
52. **Petit, C., O. Schwartz, and F. Mammano.** 2000. The karyophilic properties of human immunodeficiency virus type 1 integrase are not required for nuclear import of proviral DNA. J. Virol. **74:**7119–7126.
53. **Petit, C., O. Schwartz, and F. Mammano.** 1999. Oligomerization within virions and subcellular localization of human immunodeficiency virus type 1 integrase. J. Virol. **73:**5079–5088.
54. **Peytavi, R., S. S. Hong, B. Gay, A. Dupuy d'Angeac, L. Selig, S. Bénichou, R. Benarous, and P. Boulanger.** 1999. H-EED, the product of the human homolog of the murine *eed* gene, binds to the matrix protein of HIV-1. J. Biol. Chem. **274:**1635–1645.
55. **Pirrotta, V.** 1998. Polycombing the genome: Pcg, trxG, and chromatin silencing. Cell **93:**333–336.
56. **Priet, S., J.-M. Navarro, N. Gros, G. Quérat, and J. Sire.** 2003. Functional role of HIV-1 virion-associated uracil DNA glycosylase 2 in the correction of G:U mispairs to G:C pairs. J. Biol. Chem. **278:**4566–4571.
57. **Pruss, D., F. D. Bushman, and A. P. Wolffe.** 1994. Human immunodeficiency virus integrase directs integration to sites of severe DNA distortion within the nucleosome core. Proc. Natl. Acad. Sci. USA **91:**5913–5917.
58. **Pruss, D., R. Reeves, F. D. Bushman, and A. P. Wolffe.** 1994. The influence of DNA and nucleosome structure on integration events directed by HIV integrase. J. Biol. Chem. **269:**25031–25041.
59. **Pryciak, P. M., and H. E. Varmus.** 1992. Nucleosomes, DNA-binding proteins, and DNA sequence modulate retroviral integration target site selection. Cell **69:**769–780.
60. **Reil, H., A. A. Bukovsky, H. R. Gelderblom, and H. G. Goettlinger.** 1998. Efficient HIV-1 replication can occur in the absence of the viral matrix protein. EMBO J. **17:**2699–2708.
61. **Rietzler, M., M. Bittner, W. Kolanus, A. Schuster, and B. Holzmann.** 1998. The human WD repeat protein WAIT-1 specifically interacts with the cytoplasmic tails of β7-integrins. J. Biol. Chem. **273:**27459–27466.
62. **Satjin, D. P. E., K. M. Hamer, J. den Blaauwen, and A. P. Otte.** 2001. The Polycomb group protein EED interacts with YY1, and both proteins induce neural tissue in *Xenopus* embryos. Mol. Cell. Biol. **21:**1360–1369.
63. **Satjin, D. P. E., and A. P. Otte.** 1999. RING1 interacts with multiple Polycomb group proteins and displays tumorigenic activity. Mol. Cell. Biol. **19:**57–68.
64. **Saurin, A. J., Z. Shao, H. Erdjument-Bromage, P. Tempst, and R. E. Kingston.** 2001. A *Drosophila* Polycomb group complex includes Zeste and dTAFII proteins. Nature **412:**655–660.
65. **Scherdin, U., K. Rhodes, and M. Breindl.** 1990. Transcriptionally active genome regions are preferred targets for retrovirus integration. J. Virol. **64:**907–912.
66. **Schroder, A. R., P. Shinn, H. Chen, C. Berry, J. R. Ecker, and F. Bushman.** 2002. HIV-1 integration in the human genome favors active genes and local hotspots. Cell **110:**521–529.
67. **Schumacher, A., C. Faust, and T. Magnuson.** 1996. Positional cloning of a global regulator of anterior-posterior patterning in mice. Nature **383:**250–253.
68. **Schumacher, A., O. Lichtarge, S. Schwartz, and T. Magnusson.** 1998. The murine polycomb-group *eed* and its human orthologue: functional implications of evolutionary conservation. Genomics **54:**79–88.
69. **Schwartz, O., A. Dautry-Varsat, B. Goud, V. Marechal, A. Subtil, J. M. Heard, and O. Danos.** 1995. Human immunodeficiency virus type 1 Nef induces accumulation of CD4 in early endosomes. J. Virol. **69:**528–533.
70. **Sewalt, R. G. A. B., J. van der Vlag, M. J. Gunster, K. M. Hamer, J. L. den Blaauwen, D. P. E. Satijn, T. Hendrix, R. van Driel, and A. P. Otte.** 1998. Characterization of interactions between the mammalian Polycomb-group proteins Enx1/EZH2 and EED suggests the existence of different mammalian Polycomb-group protein complexes. Mol. Cell. Biol. **18:**3586–3595.
71. **Sherman, M. P., and W. C. Greene.** 2002. Slipping through the door: HIV entry into the nucleus. Microbes Infect. **4:**67–73.
72. **Shi, Y., E. Seto, L.-S. Chang, and T. Shenk.** 1991. Transcriptional repression by YY1, a human GLI-Kruppel-related protein, and relief of repression by adenovirus E1A. Cell **67:**377–388.
73. **Showell, C., and V. T. Cunliffe.** 2002. Identification of putative interaction partners for the *Xenopus* Polycomb-group protein Xeed. Gene **291:**95–104.
74. **Simon, J.** 1995. Locking in stable states of gene expression: transcriptional control during *Drosophila* development. Curr. Opin. Cell Biol. **7:**376–385.
75. **Smith, G. P., and J. K. Scott.** 1993. Libraries of peptides and proteins displayed on filamentous phage. Methods Enzymol. **217:**228–257.
76. **Spillane, C., C. MacDouglas, C. Stock, C. Köhler, J.-P. Vielle-Calzada, S. M. Nunes, U. Grossniklaus, and J. Goodrich.** 2000. Interaction of the *Arabidopsis* Polycomb group proteins FIE and MEA mediates their common phenotypes. Curr. Biol. **10:**1535–1538.
77. **Suzuki, Y., and R. Craigie.** 2002. Regulatory mechanisms by which barrier-to-autointegration factor blocks autointegration and stimulates intermolecular integration of Moloney murine leukemia virus preintegration complexes. J. Virol. **76:**12376–12380.
78. **Turelli, P., V. Doucas, E. Craig, B. Mangeat, N. Klages, R. Evans, G. Kalpana, and D. Trono.** 2001. Cytoplasmic recruitment of INI1 and PML on incoming HIV preintegration complexes: interference with early steps of viral replication. Mol. Cell **7:**1245–1254.
79. **Van der Vlag, J., and A. P. Otte.** 1999. Transcriptional repression mediated by the human polycomb-group protein EED involves histone acetylation. Nat. Genet. **23:**474–478.
80. **Wang, J.-Y., H. Ling, W. Yang, and R. Craigie.** 2001. Structure of a two-domain fragment of HIV-1 integrase: implications for domain organization in the intact protein. EMBO J. **20:**7333–7343.
81. **Weidhaas, J. B., E. A. Angelichio, S. Fenner, and J. M. Coffin.** 2000. Relationship between retroviral integration and gene expression. J. Virol. **74:**8382–8389.
82. **Withers-Ward, E. S., Y. Kitamura, J. P. Barnes, and J. M. Coffin.** 1994. Distribution of targets for avian retrovirus DNA integration in vivo. Genes Dev. **8:**1473–1487.
83. **Wu, X., Y. Li, B. Crise, and S. M. Burgess.** 2003. Transcription start regions in the human genome are favored targets for MLV integration Science **300:**1749–1751.
84. **Yung, E., M. Sorin, A. Pal, E. Craig, A. Morozov, O. Delattre, J. Kappes, D. Ott, and G. V. Kalpana.** 2001. Inhibition of HIV-1 virion production by a transdominant mutant of integrase interactor 1. Nat. Med. **8:**920–926.
85. **Zennou, V., C. Petit, D. Guetard, U. Nerhbass, L. Montagnier, and P. Charneau.** 2000. HIV-1 genome nuclear import is mediated by a central DNA flap. Cell **101:**173–185.
86. **Zou, S., and D. F. Voytas.** 1997. Silent chromatin determines target preference of the *Saccharomyces* retrotransposon Ty5. Proc. Natl. Acad. Sci. USA **94:**7412–7416.